

September 29, 2000

***METEOROLOGICAL MODELING OF 1996
FOR THE UNITED STATES WITH MM5***

EPA TASK ORDER NUMBER CAA689805

Prepared for

Norman Possiel, Client Representative
U.S. EPA/OAQPS

Prepared by

Donald Olerud (MCNC)
Kiran Alapaty (MCNC)
Neil Wheeler (Sonoma Technology, Inc.)

MCNC–Environmental Programs
P.O. Box 12889
Research Triangle Park, NC 27709-2889

Contents

1. Introduction	1
2. Model Description	3
3. Model Configuration.....	6
3.1 Domains.....	6
3.2 Physical Options.....	8
4. Model Inputs and Preprocessing.....	11
4.1 Preprocessing System.....	11
4.1.1 Terrain.....	11
4.1.2 Datagrid.....	12
4.1.3 Rawins.....	12
4.1.4 Interp.....	12
4.2 Lateral Boundary Conditions	12
4.3 Data Assimilation.....	13
5. Model Performance Evaluation Methodology.....	14
5.1 Data	14
5.2 Procedures	14
6. Results.....	17
6.1 General Observations	17
6.2 Spatial Analyses	17
6.2.1 Upper-Level Winds.....	17
6.2.2 Surface Winds.....	19
6.2.3 Surface-Level Temperatures.....	20
6.2.4 Surface-Level Water Vapor Mixing Ratio.....	24
6.2.5 Mixed-Layer Depths	26
6.2.6 Rainfall.....	27
6.3 Point-specific Analyses	29
6.3.1 Analyses of Meteorological Variables at Surface Observational Data Sites.....	29
6.3.2 Statistical Analyses of Meteorological Variables	31
7. Closing Observations	39
References.....	40
Appendices.....	41
Appendix A – Model Configuration File	41
Appendix B – Supplemental Plots.....	42
Appendix C – Supplemental Color Graphic Plots.....	57

1. INTRODUCTION

The Air Quality Modeling Group (AQMG) of the U.S. Environmental Protection Agency (EPA) is responsible for providing air quality modeling assessments and databases to support the development of guidance, policies, and regulations on ozone, particulate matter, toxics, and other pollutants. As part of this mission, AQMG is performing a nationwide assessment of the beneficial effects of proposed emissions reductions from cars and trucks on ozone concentrations, particulate concentrations, visibility, and acid deposition. This assessment requires developing meteorological and other related inputs to air quality simulation models, performing simulations using a regional ozone model for the western United States, and performing annual simulations of particulate matter.

The work documented in this report is referred to as “Task 2” in the original task order. The purpose of this task was to run the Pennsylvania State University (PSU)/National Center for Atmospheric Research (NCAR) Mesoscale Model version 5, or MM5^{1,2}, at 108-km and 36-km resolutions for the entirety of 1996 over the entire continental United States. This provides data necessary to drive air pollution models such as the variable-grid Urban Airshed Model (UAM-V³), the Comprehensive Air Quality Model with extensions (CAMx⁴), the Regulatory Modeling System for Aerosols and Deposition (REMSAD⁵), the Community Multi-scale Air Quality (CMAQ⁶) modeling system, or the Multiscale Air Quality Simulation Platform (MAQSIP⁷). This report documents the model inputs, model configuration, output formats, and results of these MM5 simulations.

The work to be performed under Task 2 included the following activities:

1. Developing and quality assuring all inputs to the required MM5 runs for 1996;
2. Running MM5 and quality assuring the results;
3. Delivering the outputs in electronic form; and
4. Providing documentation of the inputs, assumptions, and results.

These tasks were further broken down into eight subtasks:

1. **Acquire Data**—Purchase data from the National Center for Atmospheric Research (NCAR) and the National Climatic Data Center (NCDC) suitable for initializing, providing boundary conditions, performing four-dimensional data assimilation (FDDA), and evaluating MM5 simulations for the year 1996.
2. **Set up Domains**—Working with the Client Representative, finalize the meteorological modeling domains and set up MM5 to run on them.
3. **Configure Model**—Working with the Client Representative, finalize the configuration of MM5, including selection of boundary layer scheme and other physics options. Make modifications to MM5 to output additional variables if needed.
4. **Preprocessing**—Configure and run MM5 preprocessors.

5. **Quality Assure Inputs**—Review preprocessor logs and output files as needed to confirm that the MM5 inputs are reasonable.
6. **Run MM5**—Prepare scripts to run MM5 and archive results. Provide staff and dedicated computing resources to run MM5. Monitor MM5 execution and take corrective actions should problems arise.
7. **Quality Assure/Evaluate MM5 Output**—Review MM5 simulation logs. Visualize MM5 output and review visualizations. Calculate model performance metrics and generate graphics depicting model performance. Metrics will include bias, error, correlation coefficient, and index of agreement for wind speed and direction, temperature, cloud cover, and moisture. Graphical analyses will include comparisons of observed and modeled parameters as time-series at specific locations and contour plots of modeled values with observed values overplotted. [Note: Precipitation plots have been substituted for cloud cover, since total cloud cover is not an MM5 output variable. Given the amount of data involved, the time series requirement was deemed not to be applicable for this portion of the task.]
8. **Deliver outputs**—Copy MM5 output files to magnetic tapes in a suitable format and ship the tapes to a location in the United States, to be specified by the Client Representative.
9. **Documentation**—Prepare a report describing the inputs, configuration, and results of this task. The report will be provided in both hard and soft copy.

Three appendices are included in this report. Appendix A contains the model configuration file. Appendix B contains supplemental analysis/statistical plots. Appendix C describes the supplemental color graphic files.

2. MODEL DESCRIPTION

MM5 is one of the leading three-dimensional prognostic meteorological models available for air quality studies. It uses an efficient split semi-implicit temporal integration scheme and has a nested-grid capability that can use up to ten different domains of arbitrary horizontal resolution. This allows MM5 to simulate local details with high resolution (as fine as ~1 km), while accounting for influences from great distances, with horizontal resolutions ranging to about 200 km.

MM5 uses a terrain-following nondimensionalized pressure, or sigma-P, vertical coordinate similar to that used in many operational and research models. In the nonhydrostatic MM5, the sigma levels are defined according to an initial hydrostatically balanced reference state so that these levels are also time-invariant. The vertical sigma-coordinate is determined in terms of pressure:

$$\sigma_p = (p - p_t)/(p_s - p_t),$$

where p_s and p_t are the surface and top pressures of the model, p_t being a constant. The meteorological fields can also be used in other air quality models with different coordinate systems by performing a vertical interpolation followed by a mass-consistency reconciliation step.

The model contains several types of planetary boundary layer (PBL) parameterizations suitable for air quality applications, which represent subgrid-scale turbulent fluxes of heat, moisture, and momentum. A modified Blackadar PBL⁸ scheme uses a first-order eddy diffusivity formulation for stable and neutral environments and a nonlocal-closure scheme for unstable regimes. The Gayno-Seaman PBL⁹ scheme uses a prognostic equation for the second-order turbulent kinetic energy, while diagnosing the other key boundary layer terms. This is referred to as a 1.5-order PBL, or level-2.5, scheme¹⁰. While not specifically developed for air quality applications, the model contains the Hong and Pan Mid-Range Forecast (MRF¹¹) scheme, which has the advantage of calculating the vertical exchange coefficient, K_v , that is used as input to several common air quality models.

Initial and lateral boundary conditions are specified for real-data cases from mesoscale 3-D analyses performed at 12-h intervals on the outermost grid mesh selected by the user. Surface fields are analyzed at 3-h intervals. A Cressman-based technique is used to analyze standard surface and radiosonde observations, using the European Center for Medium-range Weather Forecasting (ECMWF) Tropical Ocean and Global Atmosphere (TOGA) analysis as a first guess. The lateral boundary data are introduced using a relaxation technique applied in the outermost five rows and columns of the coarsest grid domain.

For most traditional (1-h standard) high-ozone episodes, precipitation is not the dominant factor. On the other hand, precipitation events may have a greater impact on 8-h average ozone episodes. The MM5 contains five convective parameterization schemes (Kuo, Betts-Miller, Fritsch-Chappell, Kain-Fritsch, and Grell). It also has an explicit resolved-scale precipitation scheme that solves prognostic equations for cloud water/ice (q_c) and larger liquid or frozen hydrometeors (q_r). In addition, the model contains a short- and long-wave radiation parameterization¹².

The horizontal grid has an Arakawa-Lamb B-staggering of the velocity variables with respect to the scalars (Figure 2-1). It can be seen that the scalars (T , q , etc.) are defined at the center of the grid square, while the eastward (u) and northward (v) velocity components are collocated at the corners. The center points of the grid squares are referred to as cross points, and the corner points are dot points. Hence, horizontal velocity is defined at dot points, for example, and when data are input to the model the preprocessors do the necessary interpolations to assure consistency with the grid.

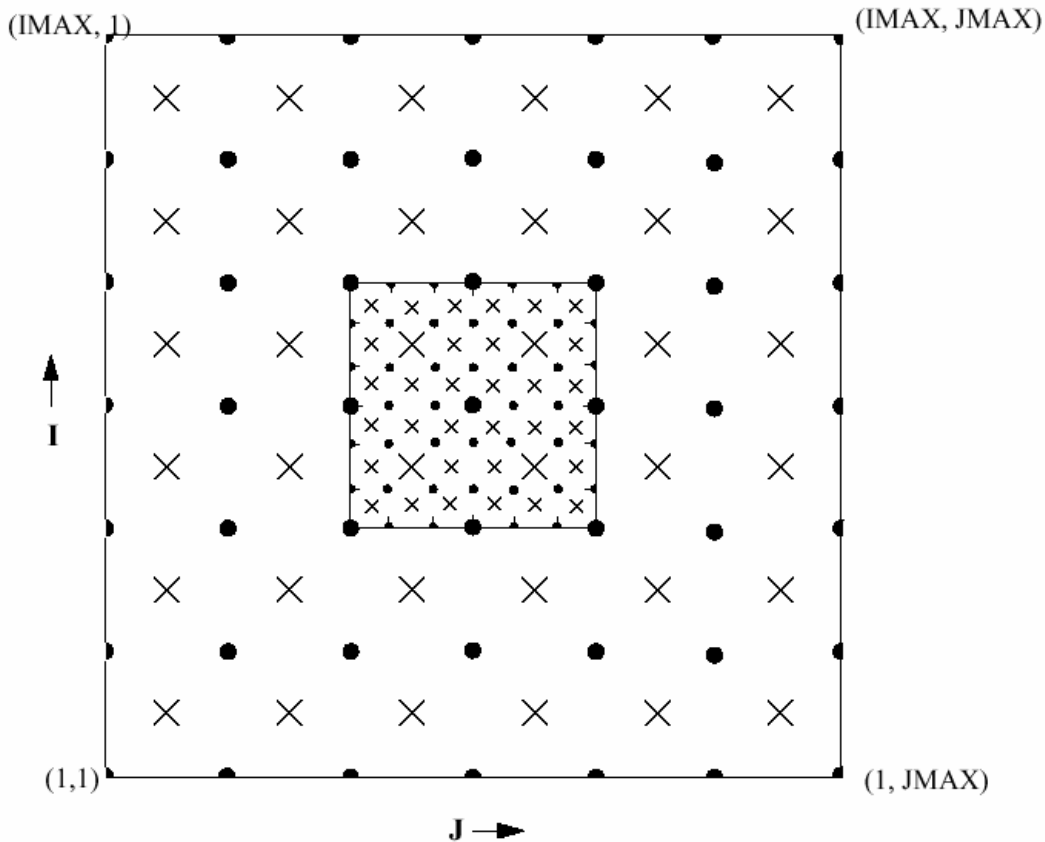


Figure 2-1. Schematic representation showing the horizontal Arakawa B-grid staggering of the dot (•) and cross (x) grid points. The smaller inner box is a representative mesh staggering for a 3:1 ratio of coarse-grid distance to fine-grid distance. (Grell et al., 1994)

The nonhydrostatic model coordinate uses a reference-state pressure to define the coordinate rather than the actual pressure that is used in the hydrostatic model. It can be seen from Figure 2-2 that σ is zero at the top and one at the surface, and each model level is defined by a value of σ . The model vertical resolution is defined by a list of values between zero and one that do not necessarily have to be evenly spaced. Commonly the resolution in the boundary layer is much finer than above, and the number of levels may vary from 10 to 40, although in principle there is no limit.

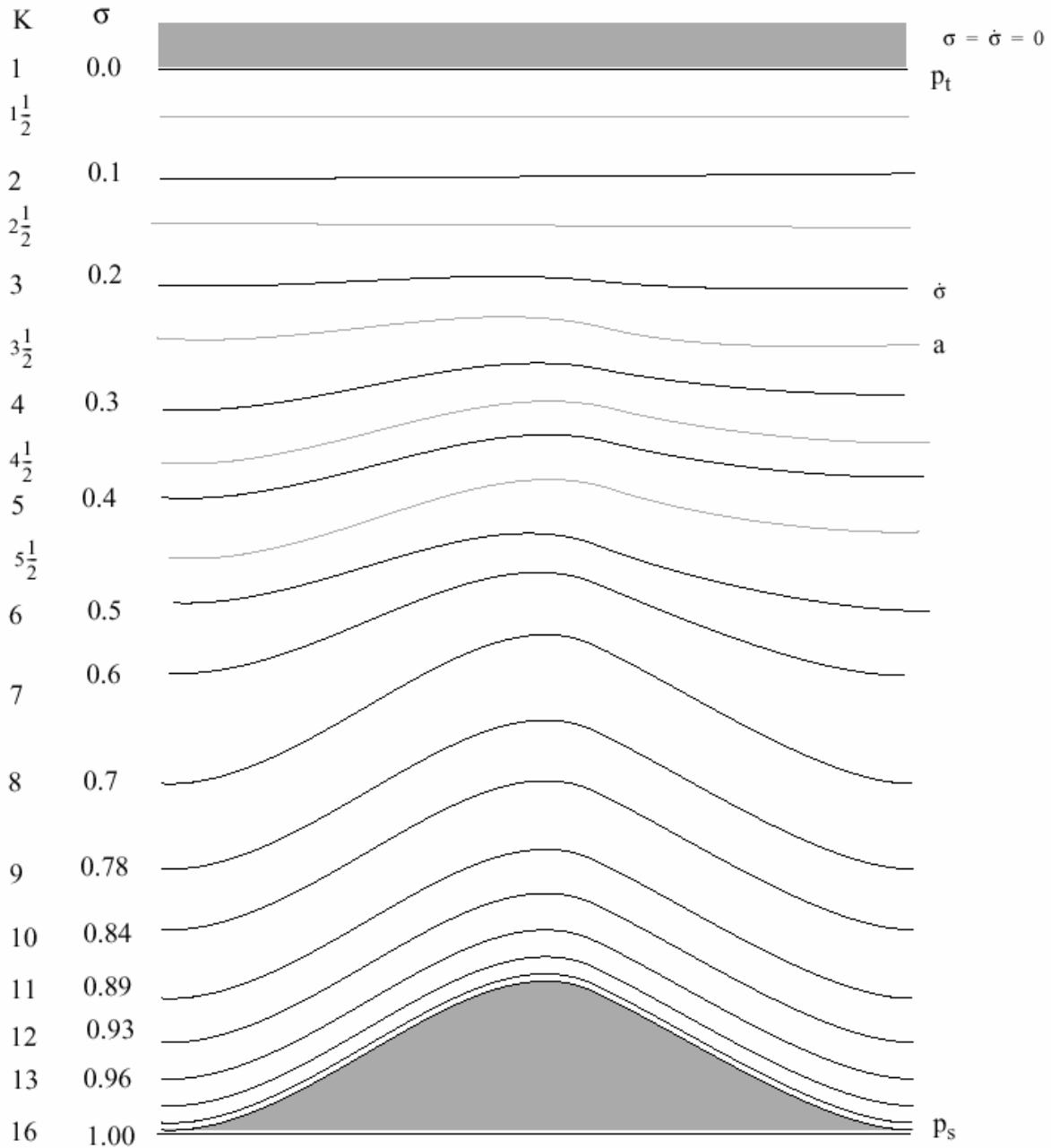


Figure 2-2. Schematic representation of the vertical structure of the model. The example is for 15 vertical layers. Dashed lines denote half-sigma levels, solid lines denote full-sigma levels. (Grell et al., 1994)

3. MODEL CONFIGURATION

For this project we used MM5 Version 2.12 with modifications to allow the output of the vertical exchange coefficient (K_v) for use in the UAM-V air quality model. We also modified MM5 to use the Meteorology-Coupler (MCPL) (<http://envpro.ncsc.org/projects/ppar/mcpl.html>) module to output selected variables in the Input/Output Applications Programming Interface (I/O API) (<http://envpro.ncsc.org/products/ioapi/index.html>) format. This allowed for rapid review of model results using MCNC's Package for Analysis and Visualization of Environmental data (PAVE) (http://envpro.ncsc.org/EDSS/pave_doc/Pave.html). The model was run for the period from 0000 UTC January 1 through 1200 UTC December 30, 1996.

3.1 DOMAINS

The domain for MM5 covers the entire United States at 108-km and 36-km resolutions, and the western half of the United States at 12-km resolution (Figure 3-1). The horizontal grid sizes are shown in Table 3-1.

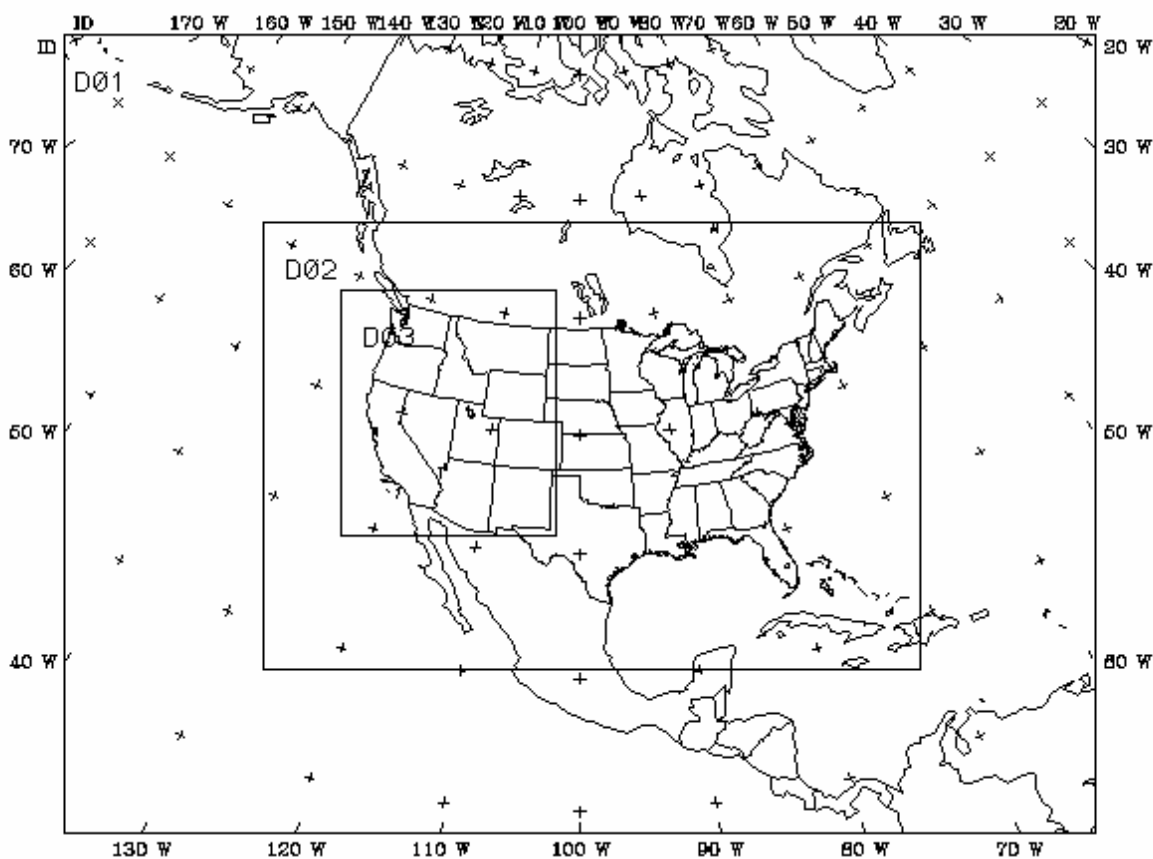


Figure 3-1. MM5 domains for the 1996 simulations.

Table 3-1. Horizontal structure of the MM5 modeling system

Domain	Resolution	E-W Cells	N-S Cells	E-W Starting Cell	N-S Starting Cell
D01	108-km	66	88	1	1
D02	36-km	114	168	15	18
D03	12-km	189	165	35	21

The vertical domain extends from the surface to the 100-mb pressure surface in 23 layers. The first layer has a thickness of approximately 38 m. The vertical structure is described in further detail in Table 3-2, where the heights are calculated using standard atmospheric conditions.

Table 3-2. Vertical structure of the MM5 modeling system

Level	Sigma	Height (m)	Pressure (mb)	Thickness (m)
0	1.000	0.0	1000.0	0.0
1	0.995	38.0	995.5	38.0
2	0.988	91.5	989.2	53.5
3	0.980	152.9	982.0	61.4
4	0.970	230.3	973.0	77.3
5	0.956	339.5	960.4	109.2
6	0.938	481.6	944.2	142.1
7	0.916	658.1	924.4	176.4
8	0.893	845.8	903.7	187.8
9	0.868	1053.9	881.2	208.1
10	0.839	1300.7	855.1	246.8
11	0.808	1571.4	827.2	270.7
12	0.777	1849.6	799.3	278.2
13	0.744	2154.5	769.6	304.9
14	0.702	2556.6	731.8	402.1
15	0.648	3099.0	683.2	542.4
16	0.582	3805.8	623.8	706.8
17	0.500	4763.7	550.0	957.9
18	0.400	6082.5	460.0	1318.8
19	0.300	7627.9	370.0	1545.5
20	0.200	9510.5	280.0	1882.6
21	0.120	11465.1	208.0	1954.6
22	0.052	13750.2	146.0	2285.1
23	0.000	16262.4	100.0	2512.1

3.2 PHYSICAL OPTIONS

The physical options selected for this configuration of MM5 include the following:

1. One-way nested grids
2. Nonhydrostatic dynamics
3. Four-dimensional data assimilation (FDDA):
 - Analysis nudging of wind, temperature, and mixing ratios
 - Nudging coefficients range from $1.0 \times 10^{-5} \text{ s}^{-1}$ to $3.0 \times 10^{-4} \text{ s}^{-1}$
4. Explicit moisture treatment:
 - 3-D predictions of cloud and precipitation fields
 - Simple ice microphysics
 - Cloud effects on surface radiation
 - Moist vertical diffusion in clouds
 - Normal evaporative cooling
5. Boundary conditions:
 - Time and inflow/outflow relaxation
6. Cumulus cloud parameterization schemes:
 - Anthes-Kuo (108-km grid)
 - Kain-Fritsch (36-km grid)
7. No shallow convection
8. Full 3-dimensional Coriolis force
9. Drag coefficients vary with stability
10. Vertical mixing of momentum in mixed layer
11. Virtual temperature effects
12. PBL process parameterization: MRF scheme
13. Surface layer parameterization:
 - Fluxes of momentum, sensible and latent heat
 - Ground temperature prediction using energy balance equation
 - 24 land use categories
14. Atmospheric radiation schemes:
 - Simple cooling
 - Long- and short-wave radiation scheme
15. Sea ice treatment:
 - Forced Great Lakes/Hudson Bay to permanent ice under very cold conditions
 - 36-km treatment keyed by observations of sea ice over the Great Lakes
16. Snow cover:
 - Assumed no snow cover for July and August
 - National Center for Environmental Prediction (NCEP) snow cover for January to June, and for September to December

A few comments on the above list: The physical parameters and options listed above were chosen for their suitability for U.S. modeling during all four seasons. However, it is important to point out that the parameterization scheme used to represent atmospheric turbulent mixing in this study (MRF) was a local-closure scheme. In this simple scheme the coefficients of vertical eddy diffusivity are estimated (not calculated) using formulations suggested by Hong and Pan¹¹. The

depth of the boundary layer is a function of the bulk Richardson number. The primary benefits of using the MRF scheme are its speed of execution, its robustness, and its ability to readily output K_v 's. A concern is that its simplicity may not allow it to perform adequately. Also, the amount of longwave cooling of the land surface will not be restricted, a situation that may lead to strong negative turbulent sensible heat fluxes over some regions at night, thereby excessively cooling the surface.

In test simulations we noticed spikes in the turbulent sensible heat fluxes as a result of oscillations in the ground/skin temperature calculations. Sometimes this error actually caused the model to fail to execute. We identified the source of error responsible for these oscillations and implemented a process time-step methodology (mitering) for time integration of ground/skin temperature calculations. This new procedure was found to be successful in eliminating spurious oscillations in boundary layer fields. Below is the code before modification, followed by the modified code.

```

IF(ISOIL.EQ.0)THEN
DTHGDT(I)=(RNET(I)-QS(I))/CAPG(I,J)-HM(I)
ELSEIF(ISLDIM.EQ.1.AND.ISOIL.EQ.1)THEN
C DETERMINE SOIL TIMESTEPS PER DELTSM FOR I-SLICE, NSOIL
NSOILI=1+IFIX(4*DIFSL/(ZS(2)-ZS(1))*DELTSM/DZS(1))
NSOIL=MAX0(NSOIL,NSOILI)

```

SLAB.88
SLAB.89
24JUN97.355
SLAB.91
25MAY98.774
SLAB.93

C...Portions Copyright 1999, MCNC--North Carolina Supercomputing Center
C... Kiran Alapaty has modified slab.F for use with MRF scheme.

```

C
IF(ISOIL.EQ.0)THEN
DTHGDT(I)=(RNET(I)-QS(I))/CAPG(I,J)-HM(I)
ELSEIF(ISLDIM.EQ.1.AND.ISOIL.EQ.1)THEN
C DETERMINE SOIL TIMESTEPS PER DELTSM FOR I-SLICE, NSOIL
NSOILI=1+IFIX(4*DIFSL/(ZS(2)-ZS(1))*DELTSM/DZS(1))
NSOIL=MAX0(NSOIL,NSOILI)
CAQM: Kiran: Ensure stability if large diffusion exists in soil layers
CAQM: particularly coarse horizontal resolution domain(s).
IF(RNET(I).GT.0.0 .and. DELTSM.GE.29.) then
DTKAY = AMIN1(30.,DELTSM)
NSOIL = NINT(DELTSM/DTKAY)
NSOIL = MAX(1,NSOIL)
END IF
CAQM: end of stable time step

```

SLAB.88
SLAB.89
24JUN97.355
SLAB.91
25MAY98.774
SLAB.93
AQMSOIL.01
AQMSOIL.01
AQMSOIL.02
AQMSOIL.02
AQMSOIL.02
AQMSOIL.02
AQMSOIL.02
AQMSOIL.02

The wintertime simulations exposed a couple of shortcomings in MM5V2.12. The snow cover fields are set at model initialization, and the snow is not “allowed” to melt or to accumulate. This sometimes results in anomalously cold (or warm) areas, depending on the synoptic situation. Of more concern is the means by which MM5 treats water bodies that are subject to freezing over in the winter. The default mode is to keep all water bodies liquid regardless of the meteorological situation. Our testing revealed that this deficiency leads to water temperatures never falling below 0°C. At times this results in an artificial “heat” low over Hudson Bay. To combat this artificial feature, we implemented a code change in MM5. If the

NMC analysis suggested snow cover over a particular water cell, and if the initial ground (skin) temperature was -5°C or less, we changed the land use category from water to snow/ice. For the 36-km grid, this methodology was only applied if the National Ice Center (NIC) charts indicated significant ice coverage over the Great Lakes for the episode in question. (See <http://www.natice.noaa.gov/greatlakes.htm>.) The code that performs this modification is included below.

```

        IF(IFSNOV(1).EQ.0)GOTO 190                                INIT.314
        DO 185 I=1,ILX                                           INIT.315
          DO 185 J=1,JLX                                           INIT.316
            IS=INT(SATBRT(I,J)+0.001)                             INIT.317
            CAQM  IF((XLAND(I,J)-1.5).GE.0)THEN                    INIT.318
              IF((XLAND(I,J)-1.5).GE.0 .and. SNOWC(I,J).LE.0.0)THEN  INIT.318
                SNOWC(I,J)=-0.01                                   INIT.319
              ELSE                                                INIT.320
                SNOWC(I,J)=SNOWC(I,J)                             INIT.321
              ENDIF                                              INIT.322
            CAQM-Kiran: Begin Mods
              IF((XLAND(I,J)-1.5).GE.0 .and. SNOWC(I,J).GT.0.0 .and.
                &  TGB(I,J).LT.268.15)THEN                        INITAQM1
                XLAND(I,J) = 1.0                                  INITAQM2
                SATBRT(I,J) = 24                                  INITAQM3
              END IF                                              INITAQM4
            CAQM-Kiran: End Mods

```

4. MODEL INPUTS AND PREPROCESSING

Various types of measured and analyzed meteorological fields are required to prepare model inputs: surface data, such as temperature, winds, and moisture; upper-air data (soundings); sea surface temperature; and global/regional analysis fields. The National Center for Environmental Prediction supplies data for the surface fields for every 3 and 6 hours, and upper-air data at 12-h resolution. The National Meteorological Center provides global and regional analysis data along with the sea surface temperature data. Under the TOGA program, the ECMWF provides global analysis fields; analysis fields are usually available at 0000 and 1200 UTC at a resolution of 2.5° on a latitude-longitude grid.

In this section, we briefly describe preprocessors and their functionalities in preparing inputs to MM5. For detailed information, the reader is referred to the MM5 system documentation available from NCAR (<http://www.mmm.ucar.edu/mm5/mm5-home.html>).

4.1 PREPROCESSING SYSTEM

There are four preprocessors that process various types of input data for use in MM5: Terrain, Datagrid/REGRID, Rawins, and Interp.

4.1.1 Terrain

The Terrain preprocessor allows the user to choose map projections, horizontal grid resolutions, the number of horizontal grid cells to be used in MM5 (and thus the domain coverage), and the number of land use categories to use in representing each of the grid cells in the domain. Inputs are available in a preprocessed format. For example, global terrain and land use data are available in the following five formats:

- 1° (~111 km)
- $30'$ (~56 km)
- $10'$ (~19 km)
- $5'$ (~9 km)
- $30''$ (~0.9 km)

In this study we used 108-, 36-, and 12-km horizontal grid resolutions to perform the model simulations. Thus, 56-, 19-, and 9-km input data were used. There are 24 categories in the U.S. Geological Survey (USGS) data to represent land use. Table 4.1 lists these land use categories. The dominant land use was used for each of the grid cells. Smoothing and desmoothing techniques were used to filter noise in the terrain data (such as $2-\Delta X$ modes). We projected the input data to Lambert-Conformal coordinates.

Table 4.1. USGS land use categories

1. Urban	2. Dry Land Crops Pasture	3. Irrigated Crops Pasture
4. Mixed Dry/Irrig. Crops Past.	5. Crops/Grassland Mosaic	6. Crops/Wood Mosaic
7. Grassland	8. Shrubland	9. Mix Shrubland/Grassland
10. Savanna	11. Deciduous Broadleaf	12. Deciduous Needleleaf
13. Evergreen Broadleaf	14. Evergreen Needleleaf	15. Mixed Forest
16. Water Bodies	17. Herbaceous Wetland	18. Wooden Wetland
19. Barren Sparse Vegetation	20. Herbaceous Tundra	21. Wooden Tundra
22. Mixed Tundra	23. Bare Ground Tundra	24. Snow or Ice

4.1.2 Datagrid

The Datagrid preprocessor is used to generate meteorological data at standard pressure levels and at all grid cells along the mapped coordinates. Typically, all the basic meteorological parameters (such as winds, temperature, relative humidity, and geopotential height) are interpolated from a latitude-longitude grid to a Lambert-Conformal grid using a two-dimensional 16-grid overlapping parabolic fit method¹³.

4.1.3 Rawins

Datagrid output is used to improve the analysis fields, since the original analysis data (TOGA/NMC) are at a very coarse horizontal resolution. Using the upper-air data, Rawins performs objective analysis, and removes erroneous observations.

4.1.4 Interp

The Interp preprocessor handles the data transformation required to go from pressure levels to model sigma-based levels. Appropriate vertical interpolation schemes are used to facilitate the proper transfer of data from pressure to sigma coordinates. This preprocessor takes in data generated by Datagrid and Rawins to create final formats of initial and lateral boundary conditions for the outermost domain (108-km grid). For the inner 36-km domain, this preprocessor is used in “back-end” mode to generate initial and lateral boundary conditions.

4.2 LATERAL BOUNDARY CONDITIONS

For the outermost domain (108-km), the lateral boundary conditions are usually available at 0000 and 1200 UTC from the Interp preprocessor. For the inner 36-km domain, lateral boundary conditions are generated for every hour via the “back-end” mode of Interp, using the 108-km results as input. During the MM5 model integration, these lateral boundary conditions are further interpolated in time to every model time-step.

4.3 DATA ASSIMILATION

We chose to use the continuous FDDA method, in which prognostic fields (winds, temperature, and water vapor mixing ratio) are continuously nudged towards respective observations. Basically, time tendencies from the analysis fields are merged with time tendencies from the model in a manner such that the model solution exhibits a smooth behavior. For each of the prognostic variables, there is an associated weighting function used in the assimilation technique. In this study, winds were nudged in the entire atmospheric column, while temperature and mixing ratio were nudged only above the PBL. The weighting coefficients for various domains used are given below:

108-km domain:	Temperature and winds: $3.0 \times 10^{-4} \text{ s}^{-1}$	Mixing ratio: $1.0 \times 10^{-5} \text{ s}^{-1}$
36-km domain:	Temperature and winds: $2.5 \times 10^{-4} \text{ s}^{-1}$	Mixing ratio: $1.0 \times 10^{-5} \text{ s}^{-1}$

5. MODEL PERFORMANCE EVALUATION METHODOLOGY

5.1 DATA

For this project we used the Techniques Development Laboratory (TDL) U.S. and Canada surface hourly observations (<http://dss.ucar.edu/datasets/ds472.0/>). These data contain most of the first- and second-order National Weather Service stations, as well as automated surface sites. While these data have been subjected to a measure of quality control, experience has shown that a few spurious reports typically remain. Time and budget constraints did not allow us to perform additional quality control on these data, so the plots that follow may show evidence of these erroneous reports. Because the erroneous reports are limited, however, the essence of the plots is unaffected. The analyses that follow focus primarily on daily averages. We included only the reports that had nonmissing data for at least 21 hours in a day; our experience with the TDL data suggests that erroneous reports are less likely to occur at stations that report regularly. We also performed analysis based on daily maximum and minimum temperatures. Again, we included only regularly reporting stations, but we also excluded maximum/minimum that was considerably higher/lower than the second highest/lowest value. For the upper-air wind plots, we modified Rawins to allow upper-air observations to be extracted. These data likewise were not quality controlled, so anomalous reports might appear on the upper-air plots that follow. It should be reiterated that MM5's quality control procedures automatically remove erroneous observations before using them in its FDDA routine.

5.2 PROCEDURES

We performed qualitative and quantitative analyses of various prognostic and diagnostic parameters obtained from the MM5 simulations. First, we qualitatively visually analyzed the spatial distributions of boundary layer parameters such as simulated winds, temperature, water vapor mixing ratio, mean sea level pressure, skin temperature, rainfall, and turbulent heat fluxes. Second, we condensed the hourly data to daily-averaged quantities, as specified above. The daily data were used to produce spatial plots of model results with observations (or model-observation differences) overlaid. To reduce the number of plots, we produced spatial plots for one time each month, and the 15th day of each month was randomly selected. Aloft, we produced once-a-month "snap shots" of the wind field at three levels; we alternated between 1200 UTC and 0000 UTC, since the lower levels could show a diurnal variation. Time series of observations/model predictions were also made at a few selected sites. Finally, we produced statistical plots for daily (CST) averaged temperature, mixing ratio, wind speed, and wind direction, as well as daily maximum and minimum temperatures. These plots contain specified model-observation averages, mean bias, mean absolute error, index of agreement, and coefficient of determination. The plots were created for the entire domain (peripheral 2-3 cells excluded), and also for the 4 subdomains shown in Figure 5.1.

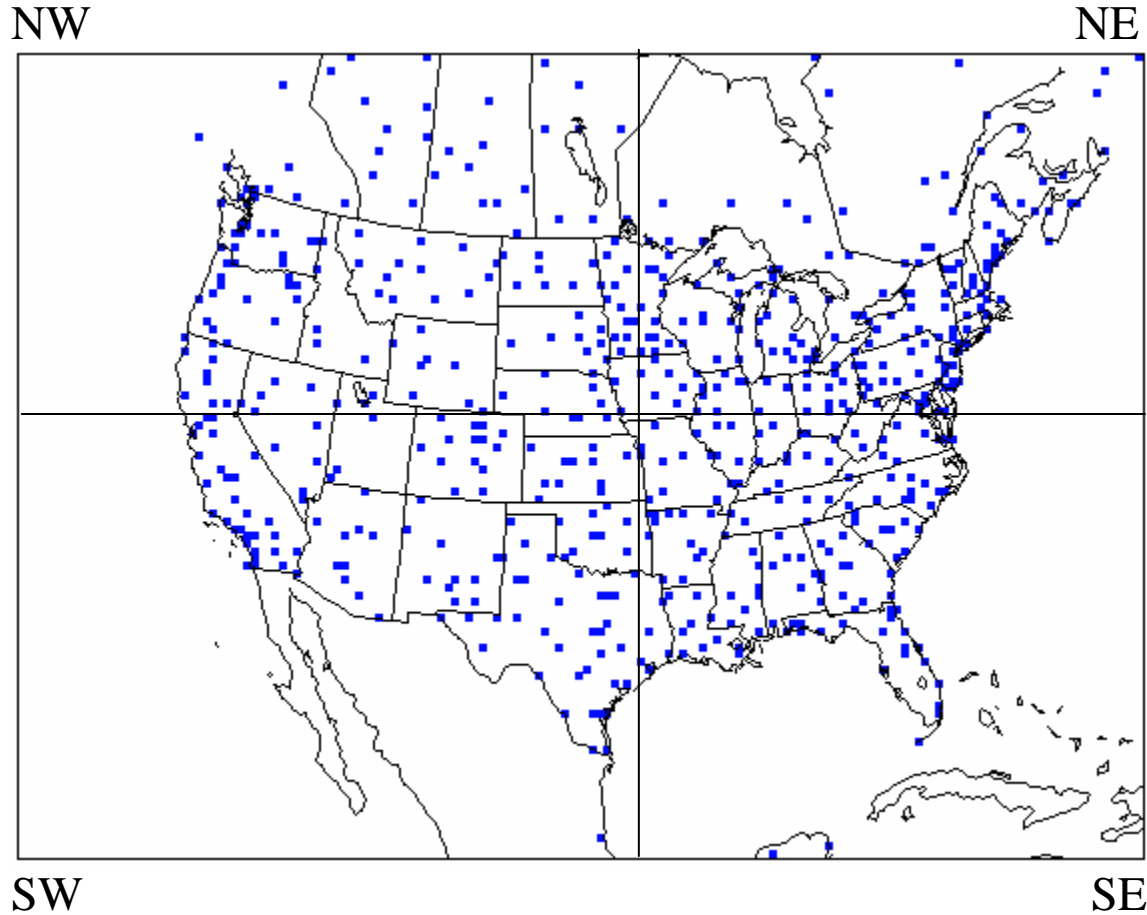


Figure 5.1. Domains for statistical plots. The full domain matches the MM5 full 36-km domain with a 3-cell buffer to the west and south, and a 2-cell buffer to the east and north. The colored cells indicate those cells with valid observations for a randomly selected day. The compass designations NW, NE, SW and SE are used to differentiate the four subdomains.

The following methodologies were used to accomplish model performance evaluation.

- PAVE—The Package for Analysis and Visualization of Environmental data is a graphical animation tool with interactive GUI capability. It is designed to assist modelers performing time series analysis, horizontal and vertical spatial analysis, and animations. Detailed information on using PAVE can be found at

http://envpro.ncsc.org/EDSS/pave_doc/Pave.html

We used PAVE to perform qualitative analysis of various diagnostic and prognostic parameters, as well as quality assurance.

- GrADS—The Grid Analysis and Display System is used to visualize modeled data overlaid with observations. We selected three model vertical levels ($L=6, 11, \text{ and } 16$),

which approximately correspond to 400, 1400, and 3400 m above ground level (AGL). Spatial plots of wind, temperature, mixing ratio, and precipitation were generated with observations (or model-observation differences) overlaid. These plots are presented in Section 6. Further details on GrADS can be obtained at <http://grads.iges.org/grads/>.

- XMgr—The XMgr is a simple and elegant graphical tool that we used to produce time series plots. More information about XMgr can be found at <http://plasmagate.weizmann.ac.il/Xmgr/>.
- Graph and NCAR graphics—Graph is an MM5 postprocessor that produces graphical images of modeled input and output data. It uses graphical software developed by NCAR. We used this postprocessor to produce sea-level pressure and 500-mb height spatial plots, and model sounding plots for preselected stations. These plots were generated daily at 0000 and 1200 UTC.

6. RESULTS

In this section we analyze the model performance. First we give a qualitative overview; then we focus on spatial analyses of specified quantities at the surface and aloft. Next we examine statistical measures of surface variables for the entire analysis domain and for the four subregions. We then examine point-specific performance using time series.

6.1 GENERAL OBSERVATIONS

During the qualitative examination of MM5 output variables, three concerns surfaced. First, the PBL heights seemed to be capped at about 2000 m. This problem is most noticeable in the summer, since PBL heights seldom approach 2000 m at other times during the year. The second concern involves lake temperatures. A problem in MM5 version 2.12 exists whenever the “24 land use” option is selected, and this problem manifests itself in the temperatures assigned to the lakes. The resulting lake temperatures are far too high, often by as much as 10°C. We did not notice any anomalous flows resulting from this error, but we have seen high temperatures and mixing ratios in the areas near these lakes. The problem affects only the Great Salt Lake within the United States, while numerous Canadian lakes (e.g., Lake Winnipeg) are affected. The Great Lakes are immune to the problem.

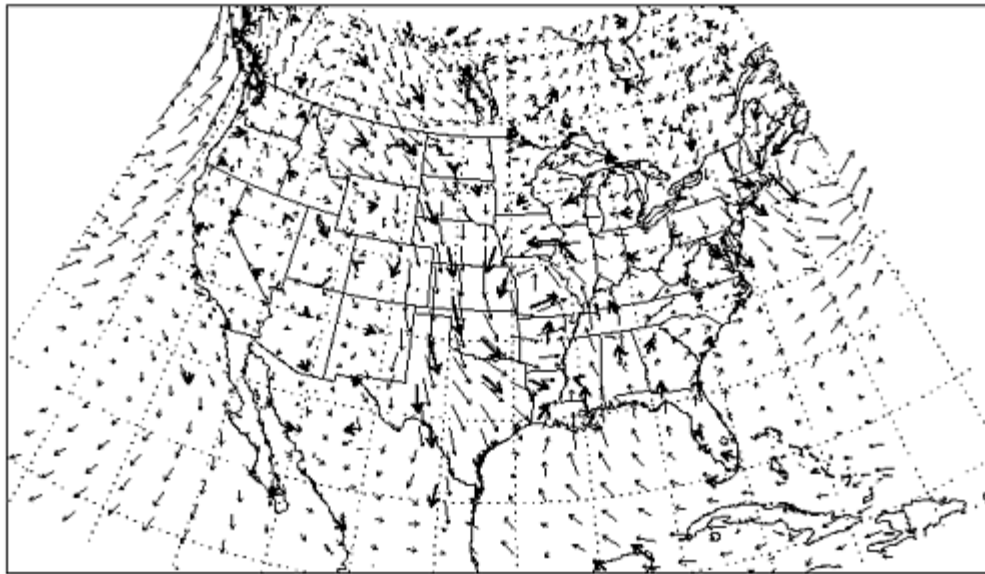
A third concern is the treatment of snow by MM5. Because MM5 version 2.12 does not have a land-surface module, the initial surface conditions remain throughout each individual 5.5-day simulation. These initial snowfields are based on the snow cover fields in the NCEP global analyses, which themselves are updated about once a week. So it is conceivable that the snow coverage used by MM5 near the end of a simulation is over ten days old from the “observed” snow coverage field. The fact that the NCEP analysis is at a 2.5° resolution (~270 km) suggests that snow could be artificially spread out over too many 36-km cells, especially in areas with significant topographical gradients.

6.2 SPATIAL ANALYSES

6.2.1 Upper-Level Winds

We focused on three aloft levels for our upper-air analyses: 0.938, 0.808, and 0.582 sigma, which approximately correspond to 400, 1400, and 3400 m AGL. These levels were chosen so that the lowest level is clearly in the middle of the boundary layer, the middle layer is towards the top of the boundary/residual layer, and the highest level is clearly above the boundary layer. Obviously there are too many days in our simulations to plot them all, so we focus only on a sampling. For the odd months (January, March, May, etc.) the plots are made at 1200 UTC on the 15th of each month. The even months are plotted at 0000 UTC on the 15th of each month. Appendix B contains all these sample plots. Figures 6.1-6.3 show the plots for April 15, 1996 (note that the images in Appendix B are larger and much easier to view).

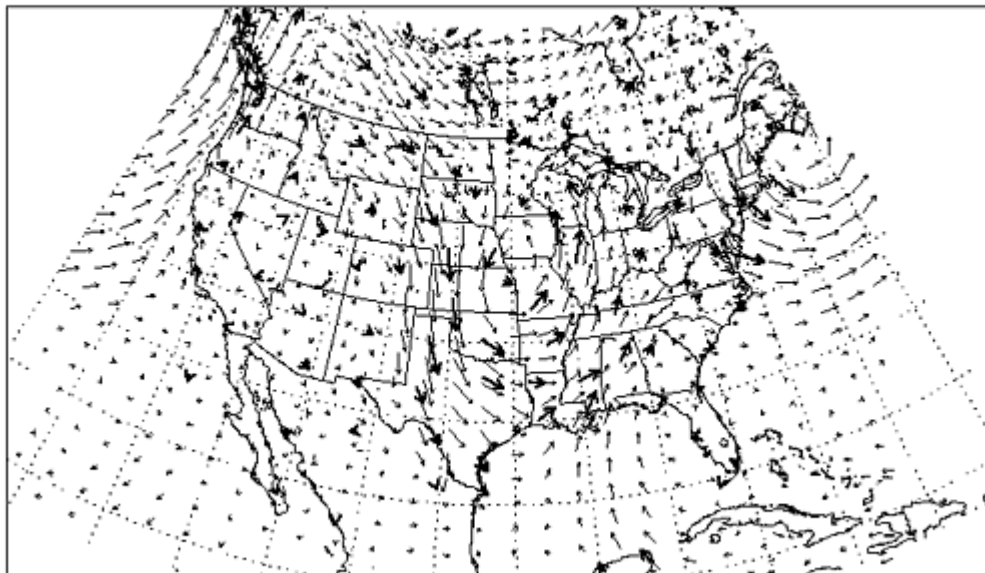
Wind Vectors (MM5, Obs at ht ~420m) 00Z 15APR96



→
16

Figure 6.1. Modeled and observed horizontal wind vectors at 0000 UTC 15 April 1996 at ~400 m AGL. Bold vectors are observations. Every fourth model vector is plotted.

Wind Vectors (MM5, Obs at ht ~1435m) 00Z 15APR96



→
20

Figure 6.2 Modeled and observed horizontal wind vectors at 0000 UTC 15 April 1996 at ~1400 m AGL. Bold vectors are observations. Every fourth model vector is plotted.

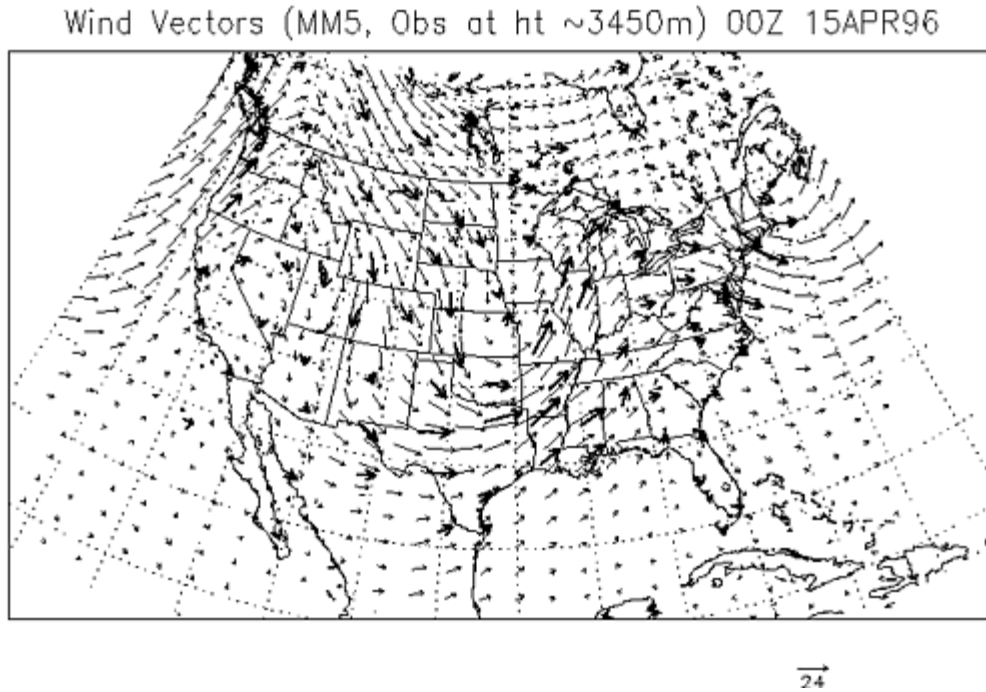


Figure 6.3. Modeled and observed horizontal wind vectors at 0000 UTC 15 April 1996 at ~3400 m AGL. Bold vectors are observations. Every fourth model vector is plotted.

Since we nudge the model to the observed upper-level winds, we expect the model and observations to show much better agreement than what we might expect to see at the surface. At each level the modeled wind directions and magnitudes agree with the observations. As expected, the performance above the boundary layer (~3400 m altitude) is best, though at no level does one see poor model-observation agreement. As expected, MM5 fully captures the large-scale synoptic flow.

6.2.2 Surface Winds

Later in this report we concentrate on a statistical analysis of surface variables, and that is the primary means of model evaluation. Still, statistics alone are insufficient to paint a complete picture of model performance. We augment the statistical information by showing a sample spatial plot of each surface variable that we have statistically analyzed, starting with surface winds. Following the pattern we used for the upper-level winds, we have included daily-averaged winds for the 15th of each month. Figure 6.4 shows the surface wind plot for April 15, 1996. Appendix B includes the plots for the 15th of each month in 1996. Figure 6.4 shows a large low-pressure system over the Great Lakes region, which MM5 resolves quite well. The strong flow behind the trailing cold front is also resolved, though it appears that MM5 has stronger winds than what were actually observed. While model output and observations show excellent directional agreement in the east, the mountainous west proves to be a different story. The model resolution of 36 km is clearly too coarse to match the observations. The hope is that at least the

synoptic flows over the mountains can be modeled, and that these flows can be hinted at in the observations. That appears to be the case for April 15.

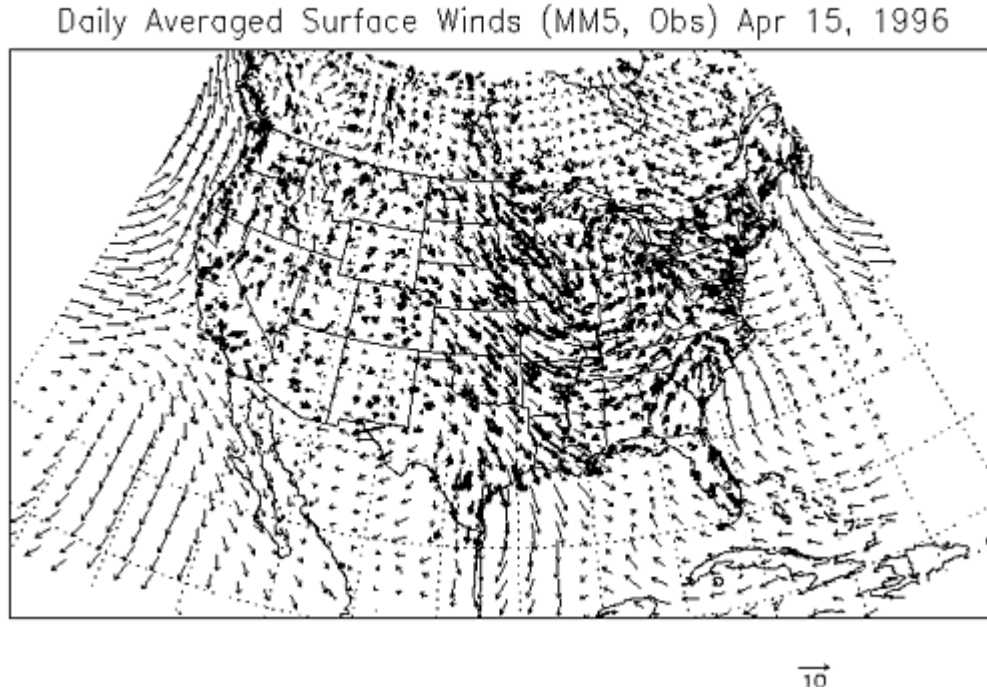


Figure 6.4. Near-surface daily-averaged modeled and observed horizontal wind vectors for April 15, 1996. Bold vectors are observations. Every third model vector is plotted.

6.2.3 Surface-Level Temperatures

We used linear interpolation between the ground and the lowest model layer to calculate temperatures at the observational height of 1.5 m. These interpolated near-surface temperatures were then averaged over each 24-hour period (0000-2300 CST). The daily maximum and minimum for each cell were also stored for later analysis. Attempting to produce model-observation plots for scalar quantities such as temperature can be quite a challenge for a domain as large as the one we used for this modeling. Even the wind plots shown earlier became cluttered at times, and we plotted only every third or fourth model vector. For smaller domains one can plot the observed value on top of model contours/tiles, but these numbers tend to cover each other up (and possibly even the model results too). It is a difficult problem. What we decided to do was to plot model-observation differences. Clearly the problem of the numbers obscuring each other exists, but we attempted to minimize this effect by colorizing these differences. Under this scheme, only absolute differences are plotted. The color scale is given in Table 6.1.

Table 6.1. Difference color scale

Difference	Color scale
# < -5	Deep Blue
-5 < # < -3	Medium Blue
-3 < # < -1	Light Blue
-1 < # < 1	White
1 < # < 3	Yellow
3 < # < 5	Orange
# > 5	Red

The difficulty with the approach given above is that it does not translate to black-and-white displays. Also the numbers themselves are not easy to read. Nevertheless it seems to be as good a way as any to plot scalar overlays. One should also keep in mind that the numbers that appear on these plots are not the same as those used in the statistical plots. For these overlay plots, all observations within the domain are plotted. The model values are interpolated to the observational points by the standard GrADS Cressman-type scheme. The statistical plots that are shown later follow a slightly different methodology. For those plots, the observations are accumulated within model grid cells. Multiple observations within a single cell are averaged. All cells with observations are paired with the corresponding model cells to produce the raw statistical data. Either approach is acceptable, especially for qualitative assessments, which is our purpose in this section.

Figure 6.5 shows the daily-averaged temperature plot for April 15. Figures 6.6-6.7 show corresponding plots for minimum and maximum temperatures. Appendix C is an accumulation of gif files containing the complete suite of figures for the 15th of each month in 1996, at a 33% larger size to facilitate viewing. Notice in the temperature plots the deleterious effects of the snowfields, especially on the maximum temperatures in Figure 6.7. Consider a west-east transect starting over the state of Washington. Modeled maximum temperatures are in the range 10-15°C, and these values are close to what the observations indicated. Eastern Washington, Idaho, and western Montana show a clear snow signature, with daily maxima just over 0°C. These low values lead to a tremendous underprediction in the model of more than 10°C. Continuing eastward, MM5 places no snow over eastern Montana, so daily maximum temperatures are 15-20°C, agreeing within 1°C to the observations. This pattern of significant temperature underpredictions over snow and more reasonable predictions in the absence of snow is a common occurrence in our modeling. Part of the problem is due to the limitations of MM5 regarding snow cover, as has already been discussed. But that does not explain everything we see in the modeling. Part of the problem is a known defect in MM5 whenever warm advection occurs over snow cover. The air quickly and sometimes anomalously cools to match the frozen surface. An additional concern is the methodology employed in our analysis. The linear interpolation technique we used means that the MM5 skin temperature is the dominant factor when we calculate the values we use to compare with observations. In the absence of snow this procedure works quite well. Over snow, however, there is likely to be a decoupling, to an extent, between the surface and the atmosphere. We have noticed that the layer 1 air temperatures in these cases could be over 5°C higher than the skin temperature during the afternoon. The differences can be much greater at the edge of the snow pack. These snow effects should be kept in mind when examining the statistical plots that are presented later in this report.

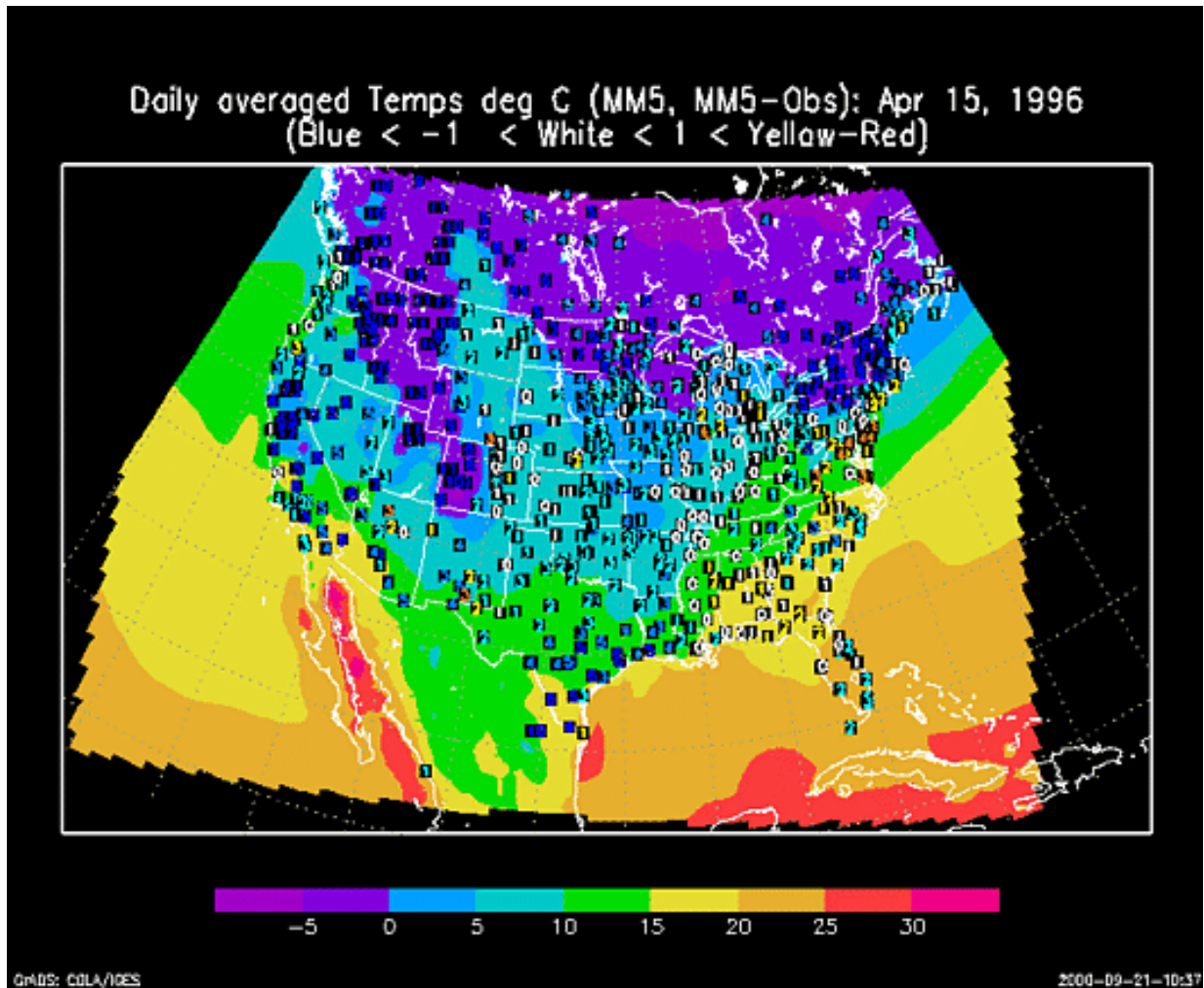


Figure 6.5. Modeled daily-averaged temperatures ($^{\circ}\text{C}$) from MM5 at 1.5 m height for April 15, 1996. The numbers are model-observation differences; blue colors represent model underpredictions, white colors indicate near 0 differences, and yellow/orange/red colors indicate model overpredictions.

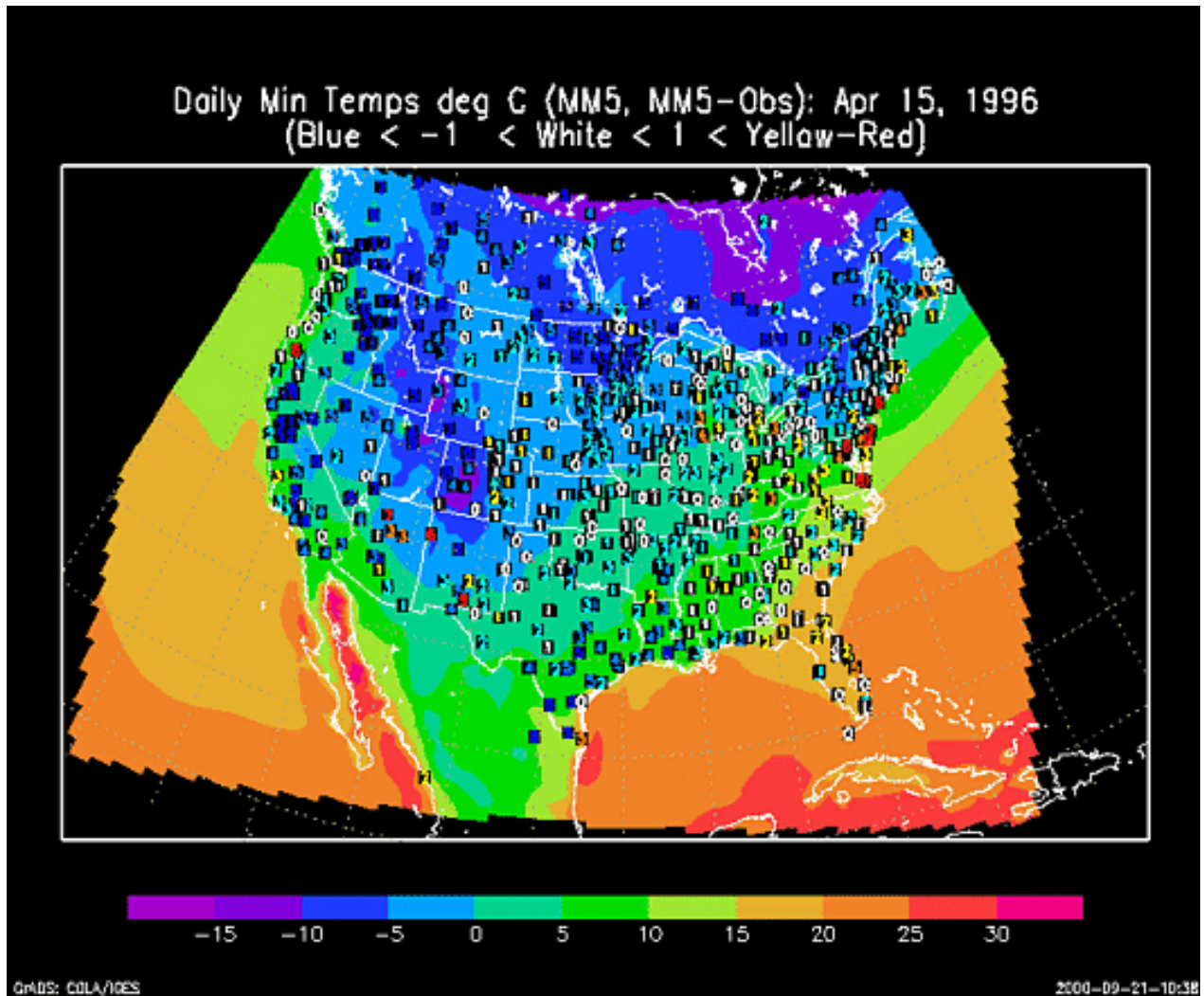


Figure 6.6. Modeled daily minimum temperatures ($^{\circ}\text{C}$) from MM5 at 1.5 m height for April 15, 1996. The numbers are model-observation differences; blue colors represent model underpredictions, white colors indicate near 0 differences, and yellow/orange/red colors indicate model overpredictions.

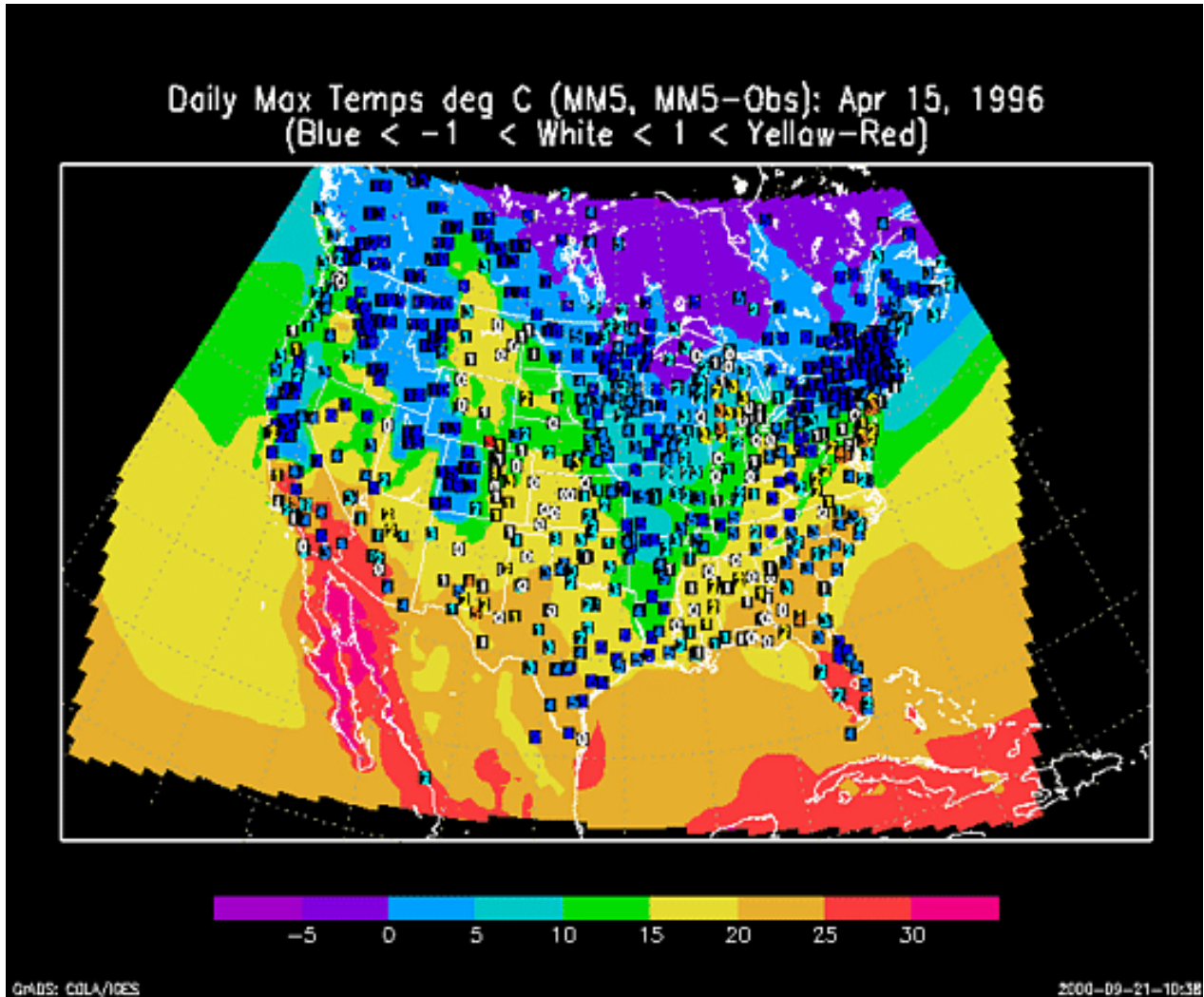


Figure 6.7. Modeled daily maximum temperatures ($^{\circ}\text{C}$) from MM5 at 1.5 m height for April 15, 1996. The numbers are model-observation differences; blue colors represent model underpredictions, white colors indicate near 0 differences, and yellow/orange/red colors indicate model overpredictions.

6.2.4 Surface-Level Water Vapor Mixing Ratio

Our analysis of “surface”-level water vapor mixing ratio followed the same procedure we used for temperature, except we performed no vertical interpolation; we simply used the lowest model layer value. Figure 6.8 shows the daily-averaged plot for our sample day. As usual, plots for the 15th of each month can be found in Appendix C. No strong moisture bias is evident, and the modeled pattern seems to agree reasonably well with the observations. Overall the water vapor mixing ratios are modeled very well throughout the year.

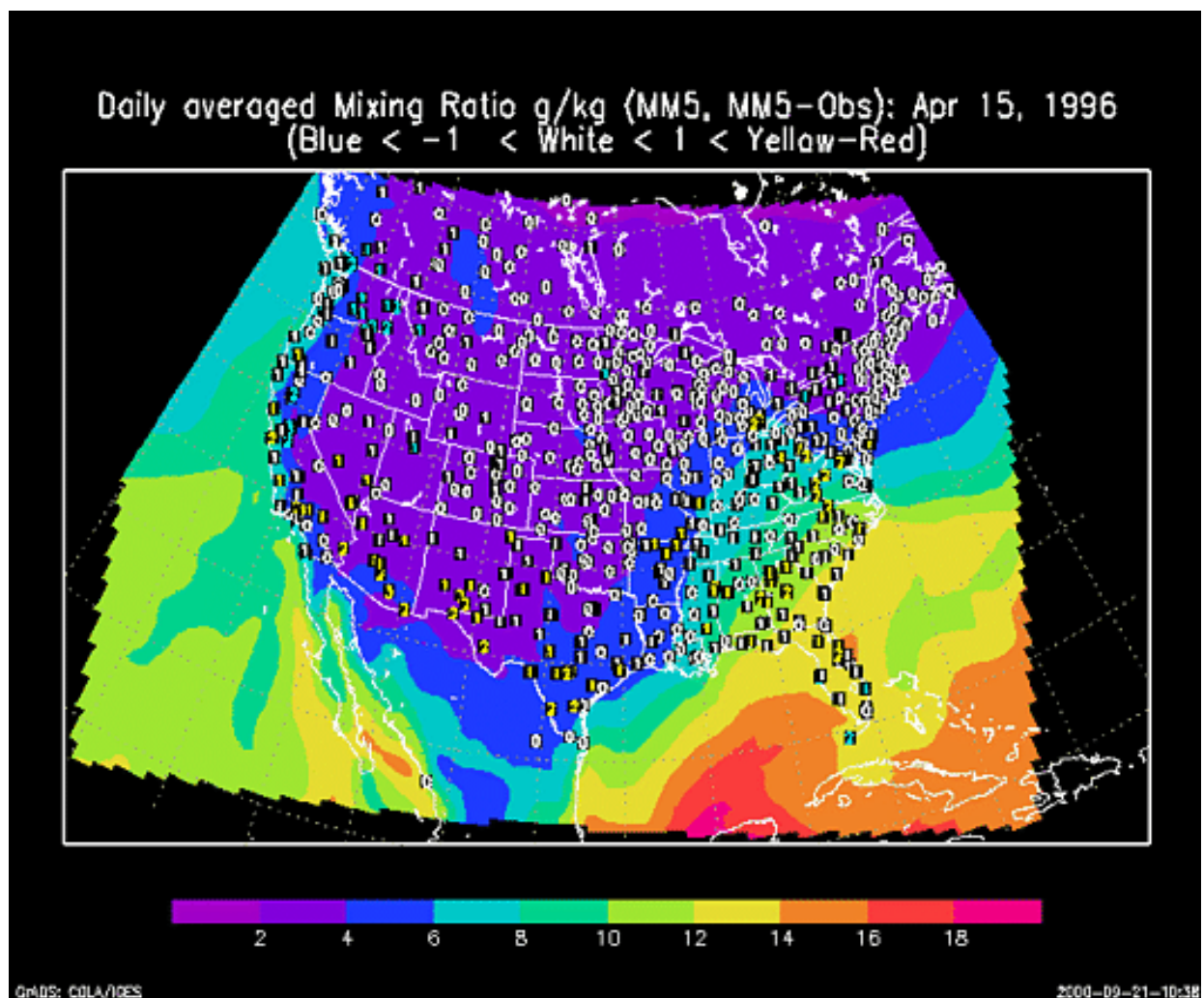


Figure 6.8. Modeled near-surface daily-averaged water vapor mixing ratios (g/kg) from MM5 for April 15, 1996. The numbers are model-observation differences; blue colors represent model underpredictions, white colors indicate near 0 differences, and yellow/orange/red colors indicate model overpredictions.

6.2.5 Mixed-Layer Depths

We have already stated our concern about the boundary layer heights output by MM5 during the simulation period (see Section 6.1). Unfortunately, routine observations of PBL heights are not directly made, so it is difficult to determine how well the MRF scheme is actually doing. To address this issue, we crudely estimated observed mixing heights from the 0000 UTC soundings. Our simple methodology assumed a potential temperature lapse rate of no more than 1.0°C/km in the mixed layer. Once the potential temperature increased at a higher rate, we assumed that it did so because it had encountered the mixed-layer capping inversion. We did try to incorporate into this methodology information from the dew point profile, but that actually seemed to cause the estimated PBL heights to deviate further from what an experienced meteorologist would estimate based on a visual examination of an observed sounding. Due to the weaknesses of this methodology, one should not place a lot of credence in the so-called PBL “observations,” especially if the value is low. Any number of factors (showers, fronts, etc.) could cause the methodology to fail. This methodology has very little chance of producing reasonable results in the winter half of the year.

It is more difficult to imagine a scenario that would cause the “observed” PBL heights to exceed the actual heights, rather than the reverse. Therefore, if MM5 predicts a mixed-layer depth of 1800 m, while the “observed” depth is 500 m, this situation should not be considered evidence that the model is flawed. However, if a couple of the “observations” indicate PBL heights in excess of 3000 m, while the model predicts 1800 m in that area, there is justification in assuming a model low bias in mixing-height prediction.

Figure 6.9 shows the maximum mixing heights for April 14, 1996 (based on 0000 UTC April 15 soundings). As has already been noted, the PBL depths are capped in the 1750-2000 m range, which appears to be a problem even this early in the year, based on the “observations” in Texas and New Mexico. The snowfield dramatically inhibits the model mixing heights. In the mountainous northwestern United States, where we previously noted significant temperature underpredictions stemming from the underlying snowfield, we note observed mixing heights well over 1000 m, much higher than that output from MM5. Otherwise the modeled mixing heights seem to reasonably correlate with the “observations.” One should also note the paucity of plotted “observations” east of the Mississippi River. This occurs whenever the observational procedure fails to calculate a value at the sounding site, and this situation is the norm during the winter. The full set of once-a-month plots of modeled versus “observed” PBL heights can be found in Appendix B.

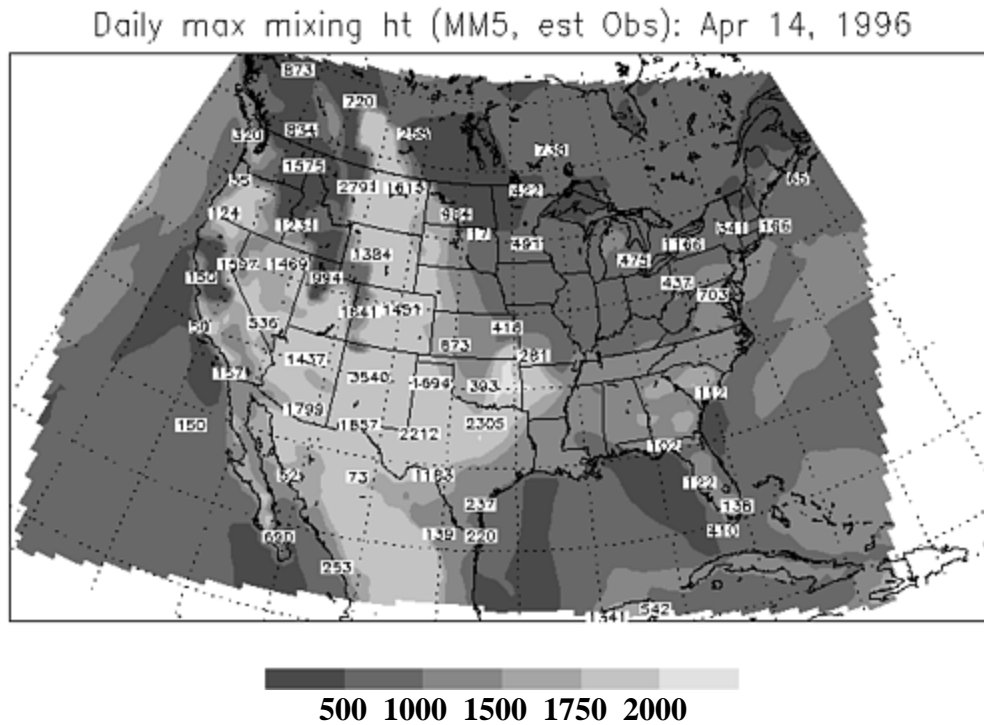


Figure 6.9. Modeled and “observed” daytime maximum depths (m) of the mixed layer for April 14, 1996.

6.2.6 Rainfall

From an air quality modeling point of view, it is important to correctly predict the geographical location of rainfall. In meteorological modeling, it is additionally important to accurately predict rainfall amounts. Figure 6.10 shows the 24-h (ending 1200 UTC April 15, 1996) accumulated precipitation amounts output by MM5 with the corresponding surface measurements. For this day the observations indicate precipitation along the extreme northwestern U.S. coast, in New England, and especially in the Mississippi Valley. MM5 also produces precipitation over these areas, while not predicting precipitation over most of the areas where no observed precipitation was reported. In general the predicted precipitation matches the observed both in area coverage and, to a lesser extent, in amount. Daily (once a month) precipitation plots can be found in Appendix B.

MM5 Precip (cm), Obs (100*cm) 24-hr total ending 12Z 15APR96

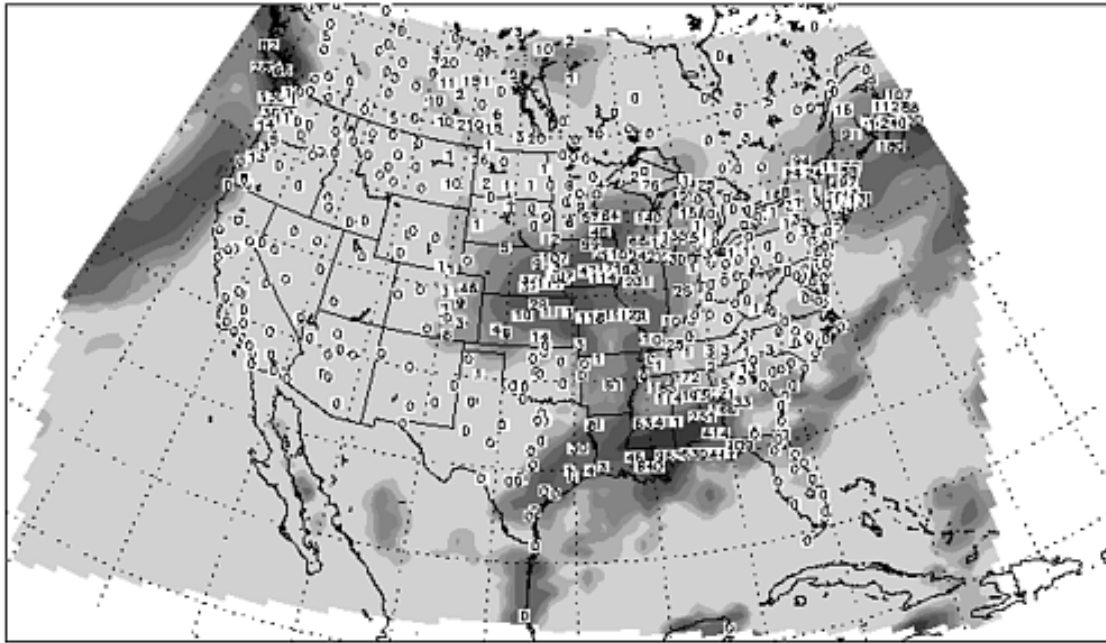


Figure 6.10. Modeled and observed accumulated rainfall for 24 hours ending 1200 UTC 15 April 1996. The numbers indicate observed rainfall in tenths of a mm/day. A “0” denotes no observed rainfall and “1” denotes trace amount of observed rainfall.

6.3 POINT-SPECIFIC ANALYSES

6.3.1 Analyses of Meteorological Variables at Surface Observational Data Sites

We selected six surface observational sites for comparison with modeled data (Table 6.2). The sites were chosen primarily for geographical balance, while also providing a sampling of the various geographical features encountered in the domain. For example, the northern sites provide information about model performance during the snow season and the transition from snow to no snow, and vice versa. The Los Angeles site gives a coastal perspective. The plots for Missoula, MT, show conditions in mountainous terrain. For each of these sites we produced time series plots (model vs. observed) for daily-averaged temperature, daily maximum temperature, daily minimum temperature, daily-averaged water vapor mixing ratio, daily-averaged wind direction, and daily-averaged wind speed. Each plot is broken into three segments of four months apiece. Also note that these observational time series represent the average of all valid observations in each cell containing a site from Table 6.2. Appendix B contains the entire suite of surface time series plots. A sample plot of daily maximum temperature for Missoula is shown in Figure 6.11. MM5 almost always underpredicts the maximum temperature for this site, especially in the late spring when the model keeps the temperatures low due to snow coverage. After the snow goes away on April 23, the performance is much improved for a couple of months. By July and August the underpredictions become more significant, often being greater than 5°C. Performance improves again for September and early October. This cell becomes snow-covered again on October 20, and the model underpredictions increase to 5-10°C for the next 15 days or so. Then the cell becomes snow-free for 10 days before becoming snow-covered the rest of the year. The last month and a half show some of the best model performance of the entire year, indicating that snow cover in and of itself does not necessarily portend poor maximum temperature performance.

The time series for the other variables and for other sites reveal more interesting information. In general, the wind direction plots show excellent agreement for the sites that are relatively geographically homogeneous (ATL, DFW, SYR, MSP). Los Angeles and Missoula show much worse performance, presumably because 36-km resolution cannot resolve the flow features adequately in coastal or mountainous environments. When viewing the wind direction plots, one should keep in mind the discontinuity at 360°/0° that sometimes causes large apparent differences in these plots. The wind speed plots show results similar to what was seen in the wind direction plots, though with slightly more error. The daily-averaged mixing ratio plots show excellent agreement for all plotted sites except Los Angeles, which again suggests a resolution problem near a large water source. Many of these sites show a tendency to slightly underpredict water vapor mixing ratio during the summer, while showing no bias the rest of the year.

The snow cover effects already discussed reveal themselves in all of the temperature plots. In the absence of snow cover, the southern sites tend to underpredict temperatures more so than the northern sites, Missoula excluded. This underprediction of temperatures is most evident in the daily maximum plots during snow cover in the spring, but it shows itself in all the plots at one time or another. The transient synoptic features such as frontal passages appear to be picked up at approximately the right times in this modeling. Surprisingly, MM5 even tends to underpredict the daily minimum temperatures.

Table 6.2. Surface observational sites

Station ID	Site name
LAX	Los Angeles, CA
DFW	Dallas/Ft Worth, TX
ATL	Atlanta, GA
MSO	Missoula, MT
MSP	Minneapolis/St Paul, MN
SYR	Syracuse, NY

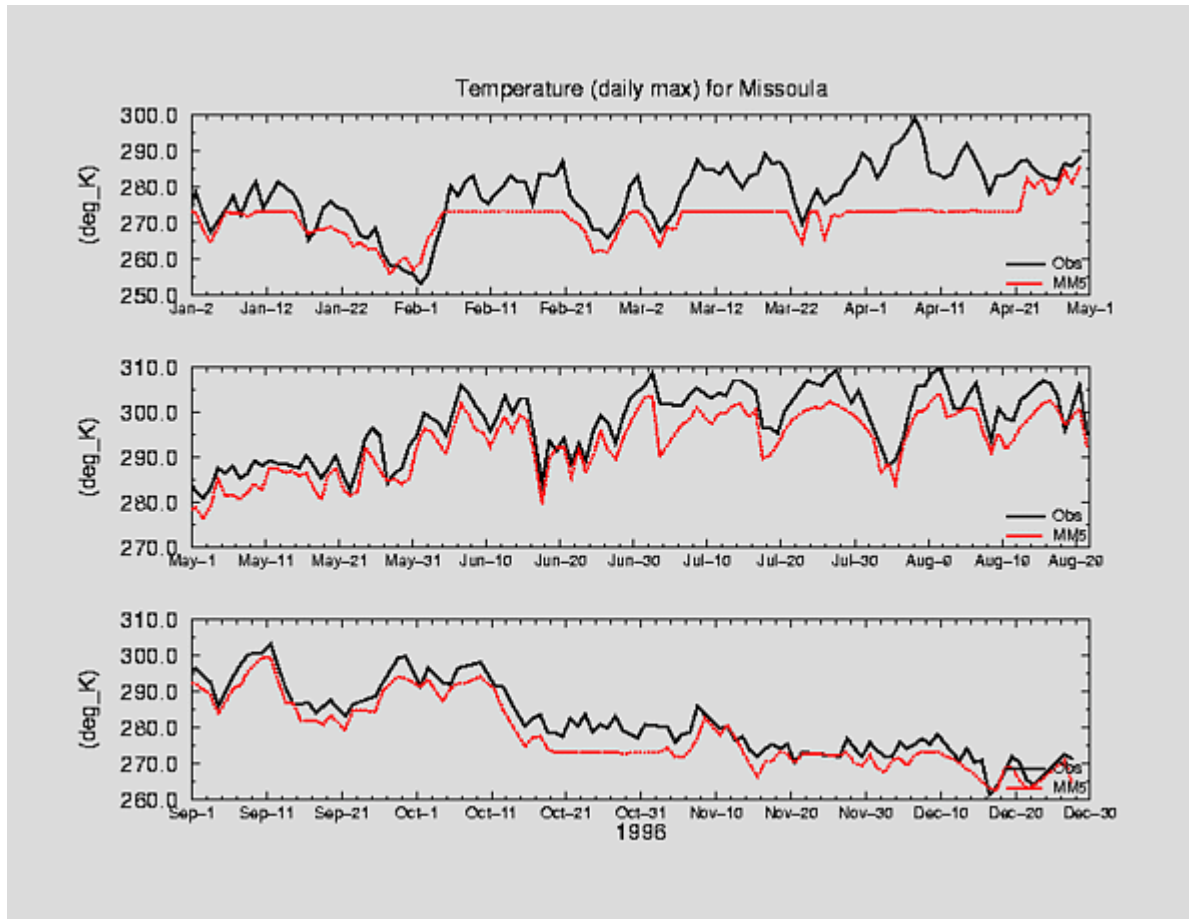


Figure 6.11. Temporal variation of modeled and observed daily maximum temperature for Missoula, MT, for the period January 2 to December 29, 1996.

6.3.2 Statistical Analyses of Meteorological Variables

To complete our model performance evaluation, we calculated and plotted a few statistical measures for the variables we have been tracking. The variables are daily-averaged wind direction and speed, daily-averaged temperature and water vapor mixing ratio, and daily maximum and minimum temperatures. The methodology is the same as what we used for the time series plots in that we are performing a cell-to-cell comparison. The observations are averaged into the cells demarcated by the model, and in the case of winds, rotated to the model coordinates. The resultant wind directions are therefore relative to the model grid, not to real-earth coordinates. Figure 5.1 contained an example of the density of cells with valid observations. It also shows the subdomains over which the following statistics were calculated. The plots are broken into four seasons, each lasting three months, starting with January. The statistics shown are (1) mean of observations and model output, (2) mean absolute error, (3) mean bias, (4) index of agreement (IA), and (5) coefficient of determination (r^2); the latter four statistics are defined below.

1. Mean Absolute Error = $\frac{1}{N} \sum |M - O|$

where N is the number of station pairs, M is the modeled value, and O is the observed value

2. Mean Bias = $\frac{1}{N} \sum (M - O)$

3. Index of Agreement = $1 - \left[\frac{N(RMSE)^2}{(|M - \bar{O}| + |O - \bar{O}|)^2} \right]$

where $RMSE$ (root mean square error) = $\left[\frac{1}{N} \sum |M - O|^2 \right]^{0.5}$

4. Coefficient of Determination (r^2) = $\frac{[\sum (O - \bar{O})(M - \bar{M})]^2}{\sum (O - \bar{O})^2 \sum (M - \bar{M})^2}$

Table 6.3 shows the statistical summary for wind direction. We calculated wind direction only whenever the observed wind speed exceeded 0.5 m/s. Wind direction statistics can be slightly misleading in that we are dealing with a discontinuous quantity. Some measures, like index of agreement, depend on the actual error divided by the total possible error range. The maximum error range is assumed to be 360°, though in actuality the maximum error is only 180°. This numerical artifact leads to higher than realistic index of agreement values. Generally speaking, model performance tends to be better in the east than in the west, presumably due to orographic effects. The summer period also tends to show slightly poorer performance than is

seen for the other seasons. This is expected, since the synoptic forcing is weakest in the summer. Overall, MM5 does a credible job in modeling the daily-averaged wind direction.

Table 6.3. Surface statistical summary for wind direction

		Jan-Mar	Apr-Jun	Jul-Sep	Oct-Dec
Wind direction (full domain)	Obs mean	203.8	190.9	187.1	196.0
	MM5 mean	202.2	190.0	186.9	194.7
	Bias	4.0	2.5	3.4	4.0
	Absolute error	23.0	22.7	24.6	21.7
	R ²	0.46	0.48	0.43	0.48
	Index of agreement	0.97	0.96	0.96	0.97
	RMSE	37.1	36.1	38.5	35.2
Wind direction (SW subdomain)	Obs mean	198.1	196.1	179.6	193.8
	MM5 mean	199.5	200.8	184.1	191.4
	Bias	6.8	6.5	6.7	7.3
	Absolute error	30.9	27.4	30.3	30.5
	R ²	0.34	0.44	0.40	0.30
	Index of agreement	0.95	0.94	0.92	0.95
	RMSE	47.8	43.2	46.6	47.1
Wind direction (SE subdomain)	Obs mean	197.1	180.6	161.0	173.8
	MM5 mean	195.6	176.6	159.7	171.7
	Bias	0.7	-0.3	0.4	0.1
	Absolute error	17.4	17.9	20.3	16.9
	R ²	0.58	0.59	0.52	0.59
	Index of agreement	0.98	0.97	0.97	0.98
	RMSE	27.0	27.7	31.0	25.8
Wind direction (NW subdomain)	Obs mean	204.2	199.0	203.5	207.0
	MM5 mean	197.6	198.5	204.2	204.4
	Bias	7.2	4.5	6.4	6.0
	Absolute error	29.4	28.1	29.6	27.0
	R ²	0.36	0.34	0.27	0.37
	Index of agreement	0.95	0.96	0.95	0.95
	RMSE	45.4	43.6	45.6	42.5
Wind direction (NE subdomain)	Obs mean	212.7	188.8	195.4	205.0
	MM5 mean	212.8	185.7	191.9	206.0
	Bias	2.3	0.2	0.9	3.0
	Absolute error	17.0	18.7	19.4	15.3
	R ²	0.55	0.60	0.54	0.63
	Index of agreement	0.98	0.98	0.98	0.98
	RMSE	27.2	28.9	29.7	23.6

Table 6.4 shows the statistical summary for wind speed. MM5 consistently overpredicts wind speed by 10-20%. This is not totally unexpected, since the MM5 value is based on a 38-m layer and the observations are made around 10 m. As we saw with wind direction, performance is better in the east than in the west. Seasonal effects vary from region to region, with the SE quadrant showing the most noticeable effect, a performance dip in the summer.

Table 6.4. Surface statistical summary for wind speed

		Jan-Mar	Apr-Jun	Jul-Sep	Oct-Dec
Wind speed (full domain)	Obs mean	3.41	3.09	2.52	3.15
	MM5 mean	3.93	3.46	2.95	3.77
	Bias	0.51	0.38	0.44	0.62
	Absolute error	1.06	0.92	0.86	1.07
	R ²	0.63	0.64	0.61	0.62
	Index of agreement	0.88	0.88	0.86	0.86
	RMSE	1.47	1.25	1.15	1.46
Wind speed (SW subdomain)	Obs mean	3.19	3.63	2.85	3.11
	MM5 mean	3.72	3.90	3.12	3.74
	Bias	0.54	0.27	0.27	0.63
	Absolute error	1.18	1.11	0.94	1.22
	R ²	0.60	0.59	0.54	0.54
	Index of agreement	0.86	0.87	0.85	0.84
	RMSE	1.63	1.51	1.27	1.69
Wind speed (SE subdomain)	Obs mean	3.41	2.72	2.07	2.99
	MM5 mean	3.78	3.12	2.56	3.58
	Bias	0.38	0.40	0.49	0.59
	Absolute error	0.86	0.77	0.77	0.92
	R ²	0.69	0.69	0.62	0.66
	Index of agreement	0.90	0.89	0.85	0.87
	RMSE	1.16	1.00	1.00	1.24
Wind speed (NW subdomain)	Obs mean	3.26	2.98	2.58	3.14
	MM5 mean	3.92	3.31	2.98	3.72
	Bias	0.66	0.33	0.40	0.58
	Absolute error	1.28	0.97	0.90	1.17
	R ²	0.57	0.61	0.60	0.61
	Index of agreement	0.85	0.87	0.86	0.86
	RMSE	1.73	1.33	1.21	1.58
Wind speed (NE subdomain)	Obs mean	3.69	3.09	2.54	3.32
	MM5 mean	4.18	3.56	3.09	3.99
	Bias	0.49	0.47	0.55	0.67
	Absolute error	0.97	0.87	0.83	0.99
	R ²	0.70	0.67	0.68	0.68
	Index of agreement	0.90	0.89	0.88	0.88
	RMSE	1.32	1.15	1.10	1.33

Table 6.5 shows the statistical summary for water vapor mixing ratio. At low mixing ratio values MM5 performs remarkably well. At higher values (>~10g/kg) MM5 tends to underpredict the observations. We believe this could be caused by the MRF PBL scheme being too efficient in its vertical mixing during hot, humid conditions. This tendency leads to seasonal and geographical patterns. The northern quadrants show better performance than the southern quadrants, and the summer period shows poorer performance than other seasons. Overall, though, MM5 does a better job modeling water vapor mixing ratio than it does any other base variable.

Table 6.5. Surface statistical summary for water vapor mixing ratio

		Jan-Mar	Apr-Jun	Jul-Sep	Oct-Dec
Mixing ratio (full domain)	Obs mean	3.5	8.0	10.9	5.0
	MM5 mean	3.6	7.6	10.1	5.0
	Bias	0.1	-0.4	-0.8	-0.0
	Absolute error	0.5	1.0	1.3	0.6
	R ²	0.91	0.92	0.86	0.93
	Index of agreement	0.98	0.97	0.95	0.98
	RMSE	0.8	1.4	1.7	0.9
Mixing ratio (SW subdomain)	Obs mean	4.1	8.0	11.5	5.7
	MM5 mean	4.5	8.3	10.8	5.8
	Bias	0.4	0.3	-0.6	0.1
	Absolute error	0.9	1.4	1.6	0.9
	R ²	0.81	0.87	0.79	0.89
	Index of agreement	0.94	0.96	0.93	0.97
	RMSE	1.2	1.8	2.0	1.2
Mixing ratio (SE subdomain)	Obs mean	5.3	11.8	14.9	7.6
	MM5 mean	5.5	10.8	13.3	7.4
	Bias	0.1	-0.9	-1.6	-0.2
	Absolute error	0.6	1.3	1.7	0.7
	R ²	0.94	0.91	0.83	0.94
	Index of agreement	0.98	0.96	0.90	0.98
	RMSE	0.9	1.6	2.0	1.0
Mixing ratio (NW subdomain)	Obs mean	2.8	5.8	8.0	3.4
	MM5 mean	2.7	5.5	7.8	3.5
	Bias	-0.0	-0.4	-0.2	0.1
	Absolute error	0.4	0.7	1.1	0.5
	R ²	0.89	0.88	0.73	0.90
	Index of agreement	0.97	0.96	0.92	0.97
	RMSE	0.6	1.0	1.4	0.7
Mixing ratio (NE subdomain)	Obs mean	2.2	6.4	9.4	3.9
	MM5 mean	2.1	6.4	9.4	3.9
	Bias	-0.1	-0.4	-0.8	-0.2
	Absolute error	0.3	0.8	1.1	0.4
	R ²	0.90	0.93	0.83	0.93
	Index of agreement	0.97	0.98	0.93	0.98
	RMSE	0.5	1.0	1.4	0.6

Table 6.6 provides the statistical summary for daily-averaged temperature. MM5 consistently shows a negative temperature bias that is most pronounced in the colder seasons. The spring/summer seasons show less bias, but also less skill. The eastern quadrants show better performance than the western quadrants, matching what we saw in the wind statistics.

Table 6.6. Surface statistical summary for daily-averaged temperature

		Jan-Mar	Apr-Jun	Jul-Sep	Oct-Dec
Temperature (full domain)	Obs mean	274.3	289.0	293.4	278.8
	MM5 mean	271.7	287.7	292.6	276.7
	Bias	-2.6	-1.4	-0.8	-2.1
	Absolute error	3.3	2.2	1.6	2.9
	R ²	0.91	0.89	0.86	0.92
	Index of agreement	0.96	0.96	0.96	0.97
	RMSE	4.2	3.2	2.3	3.6
Temperature (SW subdomain)	Obs mean	280.8	293.8	296.6	283.7
	MM5 mean	278.4	291.8	295.3	281.4
	Bias	-2.4	-1.9	-1.3	-2.2
	Absolute error	3.1	2.7	2.2	2.8
	R ²	0.86	0.81	0.80	0.90
	Index of agreement	0.94	0.93	0.93	0.96
	RMSE	4.0	3.7	2.9	3.6
Temperature (SE subdomain)	Obs mean	281.1	294.2	297.2	285.4
	MM5 mean	278.6	293.5	296.9	283.6
	Bias	-2.5	-0.7	-0.3	-1.8
	Absolute error	3.1	1.4	1.1	2.5
	R ²	0.89	0.92	0.86	0.92
	Index of agreement	0.95	0.98	0.96	0.96
	RMSE	3.9	1.8	1.4	3.1
Temperature (NW subdomain)	Obs mean	269.1	284.6	290.4	272.5
	MM5 mean	266.6	282.8	289.2	270.1
	Bias	-2.5	-1.8	-1.1	-2.4
	Absolute error	3.5	2.6	2.0	3.1
	R ²	0.90	0.81	0.80	0.92
	Index of agreement	0.96	0.93	0.94	0.97
	RMSE	4.4	3.8	2.8	3.8
Temperature (NE subdomain)	Obs mean	268.3	285.2	291.2	275.8
	MM5 mean	265.5	284.1	290.8	273.7
	Bias	-2.9	-1.1	-0.4	-2.1
	Absolute error	3.6	2.0	1.3	3.0
	R ²	0.85	0.89	0.85	0.86
	Index of agreement	0.93	0.96	0.96	0.94
	RMSE	4.4	3.0	1.7	3.7

Table 6.7 shows the statistical summary for daily maximum temperature. The statistics follow the same general pattern seen in the daily-averaged temperature statistics. A model cold bias is evident for each region for each season. The bias is most severe during the cold seasons, and the northern subdomains show more bias than do the southern subdomains. This result probably stems from the snow effects already discussed. Even considering these effects, the r^2 and IA indicate that the poorest performance occurs in the summer. The best performance for all regions is found in the October-December period.

Table 6.7. Surface statistical summary for daily maximum temperature

		Jan-Mar	Apr-Jun	Jul-Sep	Oct-Dec
Max temp (full domain)	Obs mean	279.8	294.8	299.2	283.9
	MM5 mean	276.6	293.5	298.7	281.4
	Bias	-3.3	-1.4	-0.5	-2.5
	Absolute error	4.0	2.9	2.2	3.2
	R ²	0.87	0.82	0.81	0.92
	Index of agreement	0.95	0.94	0.95	0.97
	RMSE	5.4	4.4	2.9	4.1
Max temp (SW subdomain)	Obs mean	288.2	300.9	303.3	290.4
	MM5 mean	285.3	299.6	303.1	288.2
	Bias	-2.9	-1.3	-0.1	-2.3
	Absolute error	3.9	3.1	2.6	3.2
	R ²	0.77	0.70	0.72	0.85
	Index of agreement	0.91	0.90	0.92	0.94
	RMSE	5.3	4.6	3.3	4.3
Max temp (SE subdomain)	Obs mean	286.8	299.8	302.5	290.8
	MM5 mean	283.7	299.1	302.4	288.4
	Bias	-3.1	-0.6	-0.1	-2.4
	Absolute error	3.6	2.0	1.6	2.9
	R ²	0.85	0.84	0.71	0.90
	Index of agreement	0.93	0.95	0.92	0.95
	RMSE	4.7	2.7	2.1	3.5
Max temp (NW subdomain)	Obs mean	274.2	290.3	297.0	277.1
	MM5 mean	270.5	288.2	295.8	274.2
	Bias	-3.7	-2.0	-1.2	-2.9
	Absolute error	4.6	3.5	2.5	3.5
	R ²	0.82	0.72	0.81	0.91
	Index of agreement	0.92	0.90	0.94	0.96
	RMSE	6.1	5.4	3.3	4.5
Max temp (NE subdomain)	Obs mean	272.9	290.3	296.2	279.7
	MM5 mean	269.4	288.7	295.7	277.3
	Bias	-3.5	-1.5	-0.5	-2.4
	Absolute error	4.1	3.0	2.0	3.0
	R ²	0.78	0.79	0.75	0.88
	Index of agreement	0.89	0.93	0.92	0.95
	RMSE	5.4	4.5	2.8	3.8

Table 6.8 shows the statistical summary for minimum temperature. A slight negative 1-2°C bias is seen for all regions for all of our summary periods. The snow issue is not as great a concern for minimum temperatures as it is for maximum temperatures, and the performance values have increased accordingly. Summer performance once again is poorer than the other seasons.

Table 6.8. Surface statistical summary for daily minimum temperature

		Jan-Mar	Apr-Jun	Jul-Sep	Oct-Dec
Min temp (full domain)	Obs mean	268.8	283.2	288.0	274.1
	MM5 mean	267.2	281.9	287.0	272.7
	Bias	-1.6	-1.3	-1.0	-1.4
	Absolute error	3.4	2.5	2.3	3.1
	R ²	0.87	0.87	0.77	0.87
	Index of agreement	0.96	0.96	0.93	0.96
	RMSE	4.3	3.3	3.1	4.0
Min temp (SW subdomain)	Obs mean	274.1	286.5	290.8	277.8
	MM5 mean	272.8	284.7	288.6	276.4
	Bias	-1.3	-1.9	-2.2	-1.4
	Absolute error	3.1	3.0	3.0	2.9
	R ²	0.83	0.80	0.74	0.86
	Index of agreement	0.95	0.93	0.89	0.96
	RMSE	3.9	3.8	3.8	3.6
Min temp (SE subdomain)	Obs mean	275.5	288.7	292.8	280.5
	MM5 mean	273.7	287.9	291.7	279.3
	Bias	-1.8	-0.8	-1.1	-1.2
	Absolute error	3.3	2.0	2.0	2.8
	R ²	0.85	0.88	0.75	0.85
	Index of agreement	0.94	0.96	0.91	0.95
	RMSE	4.2	2.5	2.5	3.7
Min temp (NW subdomain)	Obs mean	264.3	278.8	283.9	268.0
	MM5 mean	263.0	277.1	283.2	266.8
	Bias	-1.2	-1.7	-0.7	-1.3
	Absolute error	3.3	2.8	2.5	3.1
	R ²	0.89	0.78	0.65	0.88
	Index of agreement	0.96	0.92	0.89	0.96
	RMSE	4.2	3.7	3.3	3.9
Min temp (NE subdomain)	Obs mean	263.4	280.0	286.3	271.9
	MM5 mean	261.4	279.0	286.0	270.3
	Bias	-2.0	-1.0	-0.4	-1.6
	Absolute error	3.8	2.4	2.1	3.5
	R ²	0.78	0.86	0.66	0.74
	Index of agreement	0.93	0.96	0.90	0.92
	RMSE	4.7	3.2	2.8	4.4

Appendix B contains a full suite of statistical time series plots. From these plots it is clear that MM5 does a good job in resolving the transient synoptic features (i.e. fronts) that existed in 1996.

7. CLOSING OBSERVATIONS

In general, MM5 performed reasonably well. Major synoptic features were captured, and only a couple errors stood out. Below is our summary.

1. Near-surface temperatures are generally underpredicted.

The inability of MM5 to dynamically build/melt snowfields is the biggest concern we have with this modeling, along with the lack of proper air mass modification over these fields. The snow keeps the air mass above it from warming much above 0°C, which leads to tremendous underpredictions of temperature in the late winter/early spring. We have seen no evidence that this problem significantly affects model precipitation or wind flow. Even when snow is not present, the model consistently underpredicts temperatures (mean, maximum, and minimum).

2. PBL heights are capped at ~2000 m.

The PBL height problem seems to stem from the selection of the MRF scheme. We prefer a more sophisticated scheme, but the preferred schemes either do not output K_v 's, or they are too experimental for tasks such as this one, at least in MM5 version 2. This is primarily a summertime concern, and it affects the western states more so than the eastern states.

3. Wind fields problematic over the western states.

The 36-km resolution used in this modeling is clearly insufficient to resolve the complicated orographically-induced flows near the surface over the western United States. Elsewhere the model does a really good job in replicating the mean flow on a cell-to-cell basis. The flows aloft are modeled well everywhere.

4. Lake temperatures are too high.

MM5 version 2.12 contains a bug that causes it to sometimes misdiagnose the temperatures of certain smaller lakes. The bug only shows itself whenever the 24-category land use option is requested, as we have employed in this modeling. The effect is to create warmer-than-reasonable lake temperatures, and error is largest in the spring/summer periods. The Great Salt Lake is most susceptible to this bug, though certain Canadian lakes may also exhibit the problem. The Great Lakes are unaffected by the error.

5. Water vapor mixing ratio is modeled very well.

In general, the surface moisture fields are modeled exceptionally well. The only concern with the mixing ratio predictions is that they tend to be negatively biased during the summer in the southern states.

REFERENCES

1. Dudhia, J. A nonhydrostatic version of the Penn State/NCAR mesoscale model: Validation tests and simulation of an Atlantic cyclone and cold front. *Mon. Wea. Rev.*, **121**, 1493-1513, 1993.
2. Grell, G.A.; Dudhia, J. and Stauffer, D.R. *A Description of the Fifth Generation Penn State/NCAR Mesoscale Model (MM5)*. NCAR Tech. Note, NCAR TN-398-STR, 138 pp., 1994.
3. SAI. 1996. "User's Guide to the Variable-Grid Urban Airshed Model (UAM-V)" Systems Applications, Inc., San Rafael, California (SYSAPP-96-95/27r).
4. ENVIRON (1997) User's Guide to the Comprehensive Air Quality Model with Extensions (CAMx), Version 1.10. Environ International Corporation, Novato, CA.
5. Guthrie, P.G., C.A. Emery, M.P. Ligocki, G.E. Mansell, A.K. Kuklin and D. Gao. 1995. "Development and Preliminary Testing of the Regulatory Modeling System for Aerosols and Deposition (REMSAD)." Technical memorandum prepared for R. Scheffe, U.S. EPA Office of Policy, Planning, and Evaluation by Systems Applications International, San Rafael, California.
6. Byun, D.W. and J.K.S. Ching, Eds, "Science Algorithms of the EPA Models-3 Community Multiscale Air Quality (CMAQ) Modeling System", *EPA/600/R-99/030*, Office of Research and Development, U.S. EPA, Washington, D.C., March, 1999.
7. MCNC, The Multiscale Air Quality Simulation Platform (MAQSIP): An Overview of Model Development and Initial Applications, in preparation, 2000.
8. Zhang, D. L. and Anthes, R.A. A high-resolution model of the planetary boundary layer - Sensitivity tests and comparisons with SESAME-79 data. *J. Appl. Meteor.*, **21**, 1594-1609, 1982.
9. Gayno, G.A. *Development of a Higher-Order, Fog-Producing Boundary Layer Model Suitable for Use in Numerical Weather Prediction*. M.S. Thesis, The Pennsylvania State Univ., 104 pp.
10. Mellor, G.L. and Yamada, T. A Hierarchy of Turbulence Closure Models for Planetary Boundary-Layers. *J. Atmos. Sci.*, **31**, 1791-1806, 1974.
11. Hong S.Y. and H. L. Pan, H.L. Nonlocal boundary layer vertical diffusion in a medium-range forecast model. *Mon. Wea. Rev.*, **124**, 2322-2339, 1996.
12. Dudhia, J. Numerical study of convection observed during the winter monsoon experiment using a mesoscale two-dimensional model. *J. Atmos.Sci.*, **46**, 3077-3107, 1989
13. Chen, S., J. Dudhia, D. Gill, et al, 1995: PSU/NCAR Mesoscale Modeling System – Tutorial Class Notes. Available from NCAR (<http://www.mmm.ucar.edu/mm5>).

APPENDICES

APPENDIX A – MODEL CONFIGURATION FILE

3 domains (1st number refers to 108 km domain, 2nd number to 36 km domain, 3rd to the 12-km domain)

Sigmas

1.,0.995,.988,.98,.97,.956,.938,.916,.893,.868,.839,.808,.777,.744,.702,.648,
.582,.5,.4,.3,.2,.12,.052,.0,

KXS 23 # number of half-sigma layers

NESTIX "69,115,190," # domain heights in cells

NESTJX "89,169,166," # domain widths in cells

DIS "108.,36.,12.," # grid sizes (km)

MTHRD "1,1,2," # mother domain IDs

NESTI "1,15,35," # lower left I's of nests

NESTJ "1,18,21," # lower left J's of nests

NHYDRO = 1, #nonhydrostatic

LEVIDN "0,1,2," # level of nest for each domain

IMPHYS "5,5,5," # mixed phase ice processes

MPHYSTBL 0 # do not use look-up tables for moist physics

ICUPA "2,6,6," # Kuo,KF,KF

IBLTYP "5,5,5," # MRF

FRAD "1,1,1," # simple

ISOIL "1,1,1," # multi-layer soil temperature model (must use for MRF

pbl)

ISHALLO "0,0,0," # No shallow convection

RADFRQ "30.,20.,10.," atmospheric radiation calculation freq (in minutes)

IMVDIF 1,1,1, # moist vertical diffusion in clouds

IVQADV 1,1,1, # linear vertical moisture advection

IVTADV 1,1,1, # linear vertical temperature advection

ITHADV 1,1,1, # advection of temperature uses potential temperature

ITPDIF 1,1,1, # diffusion using perturbation temperature

ICOR3D 1,1,1, # 3D Coriolis force

IFUPR 1,1,1, # upper radiative boundary condition

IFDRY 0,0,0, # Don't do fake-dry run (no latent heating)

ICUSTB 1,1,1, # stability check for Anthes-Kuo CPS only

IBOUDY 3,3,3, # time and inflow/outflow relaxation

IFSNOW 1,1,1, # SNOW COVER EFFECTS

ISFFLX 1,1,1, # surface fluxes

ITGFLG 1,1,1, # surface temperature prediction

ISFPAR 1,1,1, # surface characteristics

ICLOUD 1,1,1, # cloud effects on radiation

ICDCON 0,0,0, # Don't use constant drag coefficients

IVMIXM 1,1,1, # vertical mixing of momentum

HYDPRE 1,1,1, # HYDRO EFFECTS OF LIQ WATER (HY run only)

IEVAP 1,1,1, # EVAP OF CLOUD/RAINWATER

TISTEP 300.,100.,36., # Adv time steps (s)

I4D 1,1,1, # GRID 4DDA RUN

```

DIFTIM    720.,720.,720.,    # 3D ANALYSIS NUDGING
          180.,180.,180.,    # SFC ANALYSIS NUDGING
IWIND     1,1,1,    # 3D ANALYSIS NUDGING of winds
          1,1,1,    # SFC ANALYSIS NUDGING of winds
GV
winds     3.0E-4,2.5E-4,1.0E-4, # 3D ANALYSIS NUDGING COEFFICIENT of
winds     3.0E-4,2.5E-4,1.0E-4, # SFC ANALYSIS NUDGING COEFFICIENT of
ITEMP     1,1,1,    # 3D ANALYSIS NUDGING of temperature
          0,0,0,    # SFC ANALYSIS NUDGING of temperature
GT
temps     3.0E-4,2.5E-4,1.0E-4, # 3D ANALYSIS NUDGING COEFFICIENT of
          0,0,0,    # SFC NUDGING of temps
IMOIS     1,1,1,    # 3D ANALYSIS NUDGING of moisture mixing ratio
          0,0,0,    # SFC ANALYSIS NUDGING of moisture mixing ratio
GQ
moisture  1.0E-5,1.0E-5,1.0E-5, # 3D ANALYSIS NUDGING COEFFICIENT of
          0,0,0,    # SFC NUDGING of moisture
IROT      0,0,0,    # GRID NUDGE THE ROTATIONAL WIND FIELD
GR        0,0,0,    # NUDGING COEFFICIENT FOR THE ROTATIONAL COMPONENT
INONBL    0,0,0,    # U WIND INCLUDE BOUNDARY LAYER NUDGING
          0,0,0,    # V WIND INCLUDE BOUNDARY LAYER NUDGING
          1,1,1,    # TEMPERATURE EXCLUDE BOUNDARY LAYER NUDGING
          1,1,1,    # MIXING RATIO EXCLUDE BOUNDARY LAYER NUDGING
RINBLW    350.,250.,150., # RADIUS OF INFLUENCE FOR SURFACE ANALYSIS (KM)
???
```

I4DI 0,0,0, # No obs nudging

APPENDIX B – SUPPLEMENTAL PLOTS

While only a small sample of plots is included in the main text, a more complete set is found here. These plots are also larger and more readable than those in the text. They do not have individual captions. Instead, a summary caption is included before each series of plots is presented. Dates and times are found in the plot labels. These plots follow:

1. Winds at ~400 m AGL on the 15th of each month (12 plots)
2. Winds at ~1400 m AGL on the 15th of each month (12 plots)
3. Winds at ~3400 m AGL on the 15th of each month (12 plots)
4. Daily-averaged surface winds on the 15th of each month (12 plots)
5. Daily maximum PBL heights on the 14th of each month (12 plots)
6. Daily accumulated rainfall on the 15th of each month (12 plots)
7. Time series for selected surface sites (36 plots)
8. Wind direction statistical time series (5 domains, 4 seasons) (20 plots)
9. Wind speed statistical time series (5 domains, 4 seasons) (20 plots)
10. Water vapor mixing ratio statistical time series (5 domains, 4 seasons) (20 plots)
11. Daily-averaged temperature statistical time series (5 domains, 4 seasons) (20 plots)

12. Daily maximum temperature statistical time series (5 domains, 4 seasons) (20 plots)
13. Daily minimum temperature statistical time series (5 domains, 4 seasons) (20 plots)

**Modeled and observed horizontal wind vectors at ~400 m AGL (Sigma=0.938; Level=6).
The plots are at 1200 UTC or 0000 UTC (alternating) for the 15th day of each month in
1996.**

Modeled and observed horizontal wind vectors at ~1400 m AGL (Sigma=0.808; Level=11). The plots are at 1200 UTC or 0000 UTC (alternating) for the 15th day of each month in 1996.

Modeled and observed horizontal wind vectors at ~3400 m AGL (Sigma=0.582; Level=16). The plots are at 1200 UTC or 0000 UTC (alternating) for the 15th day of each month in 1996.

Modeled and observed daily-averaged horizontal wind vectors near the surface. The plots are made for the 15th day of each month in 1996.

Modeled and “Observed” daytime maximum mixed-layer heights for the 14th of each month of 1996.

Modeled and observed accumulated rainfall for the 24 hours ending at 12 UTC on the 15th of each month in 1996. The numbers indicate observed rainfall in tenths of a mm/day. The “0” number denotes no observed rainfall and “1” denotes trace-amount of observed rainfall.

Temporal variation of modeled and observed daily-averaged wind direction, wind speed, surface temperature, water vapor mixing ratio, daily maximum temperature and daily minimum temperature. These sites, in alphabetical order by site name, are:

Atlanta, GA	(ATL)
Dallas/Ft Worth, TX	(DFW)
Los Angeles	(LAX)
Minneapolis/St Paul, MN	(MSP)
Missoula, MT	(MSO)
Syracuse, NY	(SYR)

Daily-averaged wind direction statistical plots. The plots represent the temporal variation of (a) domain-averaged modeled and observed means, (b) absolute error and bias, and (c) index of agreement and coefficient of determination. The plots are in seasonal segments, and they are created for the domain as a whole and for four subdomains.

Daily-averaged wind speed statistical plots. The plots represent the temporal variation of (a) domain-averaged modeled and observed means, (b) absolute error and bias, and (c) index of agreement and coefficient of determination. The plots are in seasonal segments, and they are created for the domain as a whole and for four subdomains.

Daily-averaged water vapor mixing ratio statistical plots. The plots represent the temporal variation of (a) domain-averaged modeled and observed means, (b) absolute error and bias, and (c) index of agreement and coefficient of determination. The plots are in seasonal segments, and they are created for the domain as a whole and for four subdomains.

Daily-averaged surface temperature statistical plots. The plots represent the temporal variation of (a) domain-averaged modeled and observed means, (b) absolute error and bias, and (c) index of agreement and coefficient of determination. The plots are in seasonal segments, and they are created for the domain as a whole and for four subdomains.

Daily maximum temperature statistical plots. The plots represent the temporal variation of (a) domain-averaged modeled and observed means, (b) absolute error and bias, and (c) index of agreement and coefficient of determination. The plots are in seasonal segments, and they are created for the domain as a whole and for four subdomains.

Daily minimum temperature statistical plots. The plots represent the temporal variation of (a) domain-averaged modeled and observed means, (b) absolute error and bias, and (c) index of agreement and coefficient of determination. The plots are in seasonal segments, and they are created for the domain as a whole and for four subdomains.

APPENDIX C – SUPPLEMENTAL COLOR GRAPHIC PLOTS

A file containing color gifs is available. It is a tar file named gifs96.tar which contain 48 gif files. These files show the model fields with model-observation differences overlaid. There are four categories of plots:

- 1) Daily averaged temperature (tavg_01.gif, tavg_02.gif, ..., tavg_12.gif)
- 2) Daily maximum temperature (tmax_01.gif, tmax_02.gif, ..., tmax_12.gif)
- 3) Daily minimum temperature (tmin_01.gif, tmin_02.gif, ..., tmin_12.gif)
- 4) Daily averaged water vapor mixing ratio (qavg_01.gif, qavg_02.gif, ..., qavg_12.gif)

The plots are made for the 15th of each month, with the number in each file representing a particular month. (01=Jan, 02=Feb, etc...) The differences follow a color scale represented in the following table:

Difference color scale

Difference	Color scale
# < -5	Deep Blue
-5 < # < -3	Medium Blue
-3 < # < -1	Light Blue
-1 < # < 1	White
1 < # < 3	Yellow
3 < # < 5	Orange
# > 5	Red